

# 激光扫描共聚焦荧光显微镜技术及其在地球生物学中的应用

郝立凯<sup>1,2</sup> 郭圆<sup>1</sup> 江娜<sup>1</sup> 李阳<sup>3,4</sup> 刘承帅<sup>1,2</sup>

1. 中国科学院 地球化学研究所 环境地球化学国家重点实验室, 贵阳 550081; 2. 中国科学院 第四纪科学与全球变化卓越创新中心, 西安 710061; 3. 中国科学院 地球化学研究所, 月球与行星科学研究中心, 贵阳 550081; 4. 中国科学院 比较行星学卓越创新中心, 合肥 230026

**摘要:** 光学显微镜作为生命科学研究中的必要手段, 经过近 400 年的发展其性能已得到显著提升。激光扫描共聚焦荧光显微镜成像技术的出现, 使得生物体微观三维结构的观察成为可能, 与荧光探针技术的结合更是实现了生物样品从定性到原位定量分析的质的飞跃, 同时还可提供生物体微观立体的成分结构信息。本文介绍了激光扫描共聚焦显微镜和荧光探针技术的发展现状、原理及应用方案, 列举了该技术在地球生物学领域的主要应用。基于此提出了激光扫描共聚焦显微镜成像技术改进的方向, 指出多种显微平台技术联用对生命科学的积极效应, 最终实现地球生物学的长足发展。

**关键词:** 激光扫描共聚焦荧光显微镜; 荧光探针; 地球微生物学; 古生物学

中图分类号: P52; Q91-3 文章编号: 1007-2802(2020)06-1141-32 doi: 10.19658/j.issn.1007-2802.2020.39.091

## Confocal Laser Scanning Microscopy and its Application in Geobiology

HAO Li-kai<sup>1,2</sup>, GUO Yuan<sup>1</sup>, JIANG Na<sup>1</sup>, LI Yang<sup>3,4</sup>, LIU Cheng-shuai<sup>1,2</sup>

1. State Key Laboratory of Environmental Geochemistry, Institute of Geochemistry, Guiyang 550081, China;

2. CAS Center for Excellence in Quaternary Science and Global Change, Xi'an 710061, China;

3. Center for Lunar and Planetary Sciences, Institute of Geochemistry, Chinese Academy of Sciences, Guiyang 550081, China;

4. Center for Excellence in Comparative Planetology, Chinese Academy of Sciences, Hefei 230026, China

**Abstract:** As an essential tool in life science research, the performance of optical microscopy has been remarkably improved over the past 400 years. The emergence of confocal laser scanning microscopy (CLSM) has made it possible to observe the high-resolution three-dimensional microscopic structures of organisms. The combination of CLSM and fluorescent probe technology has achieved the qualitative leap from the qualitative analysis to the quantitative in-situ structural, morphological and compositional characterization of biological samples. Here we have introduced the current states of development, principles and applications of confocal laser scanning microscope and fluorescent probe technology, especially introduced the applications in the field of geobiology. We then have proposed several directions for improving performances of the CLSM and the combination of CLSM with multiple microscopies, to further facilitate their applications in life sciences and to finally advance the development of geobiology.

**Key words:** confocal laser scanning microscopy; fluorescent probe; geomicrobiology; paleobiology

## 0 引言

光学显微镜分析是一门传统的技术学科, 伴随着光学元器件、计算机技术、自动化控制、化学材料

学的发展而逐步完善 (Fernández-Suárez and Ting, 2008)。以光学显微镜主导的微区观察和分析一直以来都是生命科学、地球科学、环境科学研究不可或缺的技术手段, 特别是对生命活动代谢功能相关

收稿编号: 2020-140 2020-08-20 收到 2020-09-07 改回

基金项目: 中国科学院 B 类战略性先导专项课题 (XDB40020300, XDB41000000); 国家重点研发计划课题 (2018YFC1802601); 中国科学院启动经费 (2017-020); 国家自然科学基金项目 (41877400); 环境地球化学国家重点实验室开放课题 (SKLEG2018911); 微生物技术国家重点实验室开放课题 (M2017-01)

第一作者简介: 郝立凯 (1980-), 男, 研究员, 研究方向: 重金属微生物地球化学与环境分析显微镜学。E-mail: haolikai@mail.gyig.ac.cn

的微观结构(Alberts et al., 2002)、金属元素生物地球化学行为过程微观机制和与微生物的相互作用(Hao et al., 2016)、环境介质微观结构组成和变化等研究,发挥着越来越重要的作用。目前,光学显微镜的总体发展趋势是多模式多维多尺度原位成像(Caplan et al., 2011),特别是激光扫描共聚焦显微镜(Paddock and Eliceiri, 2014)结合荧光探针标记技术(Waggoner et al., 2013)在对生物目标分子的精确定位(Gould et al., 2008)等方面具有独到的优势。尽管目前成熟的遗传和化学荧光探针基本能够满足大部分生命科学成像分析(Cavaliere et al., 2016),但基于荧光标记的激光扫描共聚焦显微镜(Kaestner, 2013)则更加依赖于荧光探针的开发(Fernández-Suárez and Ting, 2008; Baker, 2011)。荧光探针的飞速发展必将拓展激光扫描共聚焦显微镜可分析目标分子的范围和领域(Daly et al., 2012),特别是拓展其在重金属微生物地球化学微观过程和行控制机制等地球微生物学方面的应用。

显微镜技术越来越趋于精微定量分析。现代微生物学研究对荧光显微镜的要求是更精确、更快速定量分析,这一需求促进了荧光显微镜从定性到定量质的飞跃(Fricker et al., 2006; Gitai, 2009)。这包括选择适合定量分析的荧光探针(Okumoto et al., 2012),确定定量荧光分析的技术,保证成像过程中介质的稳定性,最终实现对生物学影像数据的定量分析(Ono et al., 2001; Meijering and Cappellen, 2007)。荧光标记技术结合成熟的光学显微镜技术使活细胞成像成为现实(Stephens and Allan, 2003)。微生物微环境研究在技术方面要求高分辨率的原位非破坏无扰动的在线分析(Wessel et al., 2013),需要同时检测两三个化学组分的荧光多标记技术或多功能荧光探针(Stich et al., 2010),这不仅需要激光扫描共聚焦显微镜实现高分辨率的定量分析(Vukojević et al., 2008),还对高通量荧光显微镜成像等方面提出了新的要求(Pepperkok and Ellenberg, 2006)。在光路和技术方面,扫频场激光(Castellano-Muñoz et al., 2012)、脉冲激发(De and Goswami, 2009)和光流技术(Delpiano et al., 2012)等先进技术可以提高激光扫描共聚焦显微镜的性能。

激光扫描共聚焦显微镜已发展成为一项成熟的高级光学显微镜技术,被广泛应用于生命科学、地球科学、环境科学研究的诸多领域(Pawley, 2006),并成功为这些学科领域的一些关键科学问题提供了直接的证据(Turillazzi et al., 2008)。通过

对目标物质的化学或遗传荧光标记,荧光显微镜特别是激光扫描共聚焦显微镜可以对生物学结构和过程进行精确的表征(Földes-Papp et al., 2003)。激光扫描共聚焦显微镜突破了电子显微镜的局限,可以避免样品制备过程中带来的原位信息丢失,如样品制备过程会造成生物膜的丢失(Chang and Rittmann, 1986)。任何单一的样品制备方法都不能完全保证保持样品的初始结构(Dohnalkova et al., 2011; Zeitvogel et al., 2017)。激光扫描共聚焦显微镜很早就被用于微生物学研究(Caldwell et al., 1992),在生物量测定(Solé et al., 2009)、微生物胞外多糖物质的微观分析(Chen et al., 2006)、细菌和EPS的空间关系(Kawaguchi and Decho, 2002)等方面都显示出巨大的潜力和优势。同时,该技术还被用于真菌学(Spear et al., 1999)、土壤微生物(Li et al., 2004)、海洋蓝藻(Tashyreva et al., 2013)等微生物学研究的多个分支学科和领域。该技术还能够提供微观立体结构的化学组成,如脂质(Chansawang et al., 2016)、胞外多糖(Lawrence et al., 2016b)及微生物种群的(Valle et al., 2015)空间分布和定量分析等方面的数据。

## 1 激光扫描共聚焦显微镜技术

### 1.1 发展历史

光学显微镜出现有近400年的历史,随着技术改进和理论发展,它已成为科学研究不可或缺的技术手段和工具。激光扫描共聚焦显微原理是由美国科学家Marvin Minsky于1957年提出的,但直到20世纪80年代后期,随着现代光学、视频、计算机等技术的发展,激光扫描共聚焦显微技术(CLSM)才逐渐成熟(图1)(Croft, 2006; Hawkes and Spence, 2007; Paddock and Eliceiri, 2014)。

CLSM通过非破坏性的光学三维切片扫描,记录源自反射、自体荧光、报告基因/荧光蛋白、与特异性靶结合的荧光染料或与荧光染料结合的其他探针信号,准确地通过可视化技术展示确定活的生物膜原位三维结构而进行半定量和/或定量分析(Staudt et al., 2004)。激光扫描共聚焦显微镜提供了微米尺度原位成像工具,可用于原初、液相条件下的生物膜的三维结构、化学组成、动态变化和生物活性。特别是与新开发的能够展示生物膜结构、化学目标专一性和扩散特异性荧光探针组合时,CLSM的优势更加突出(Bridier and Briandet, 2014; Neu and Lawrence, 2014a, 2015)。

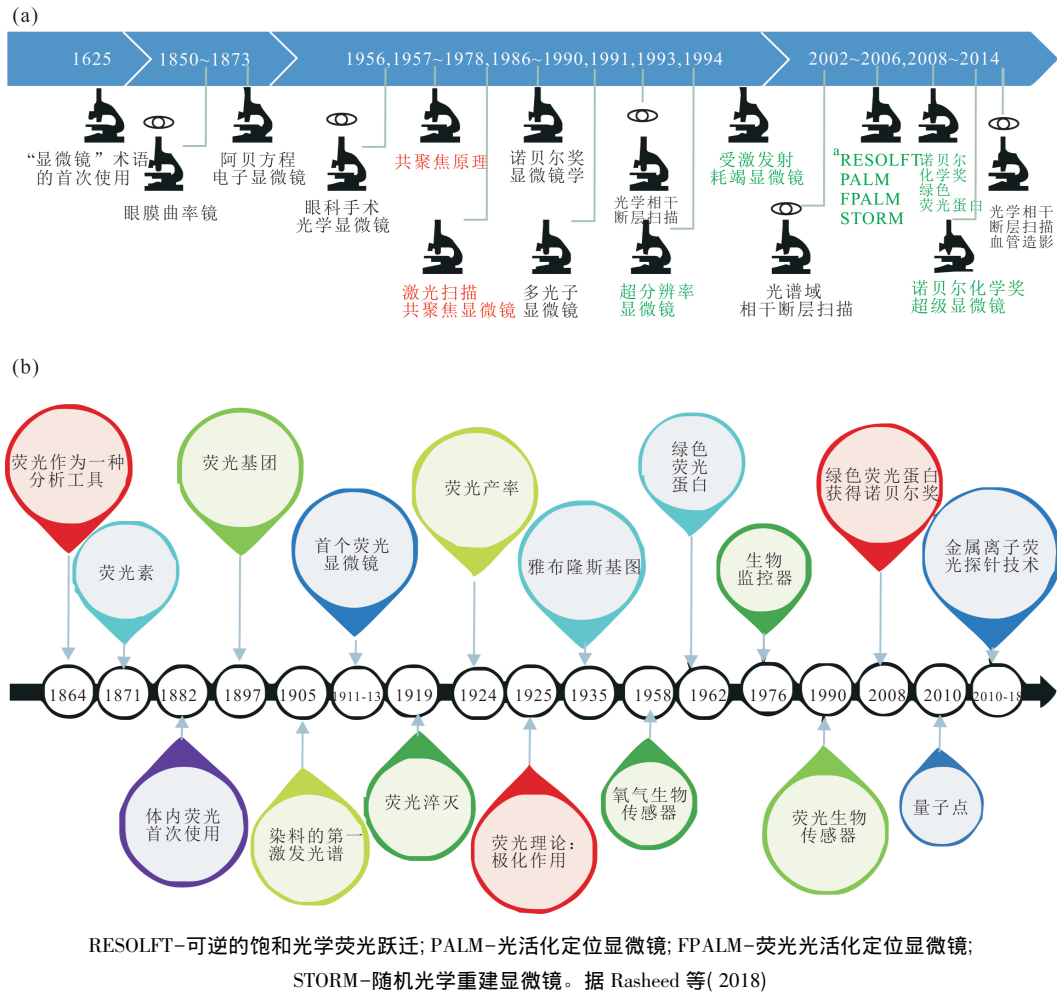


图 1 显微镜 (a) 和荧光探针 (b) 发展的主要里程碑和重要成就

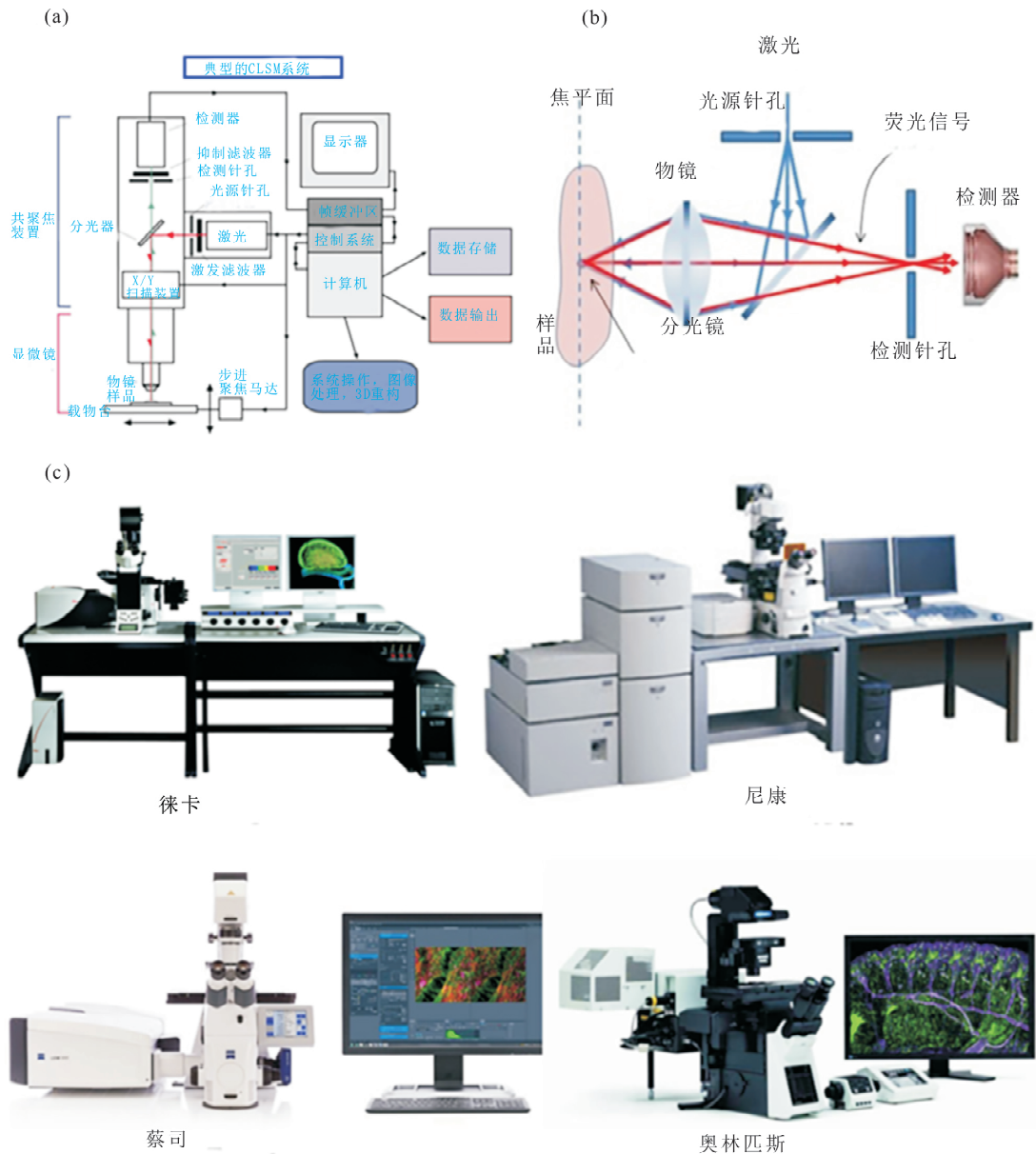
Fig.1 Major milestones and important achievements in the development of microscope (a) and fluorescent probe (b)

### 1.2 组成和原理

激光扫描共聚焦显微镜系统包括激光光源、配备激发/抑制滤波器-分光器-光源/检测针孔荧-检测器的共聚焦扫描系统、配备微步进马达的荧光显微镜、计算机控制系统和图像存储处理输出系统 (图 2a) (Paddock and Eliceiri, 2014)。用于激发荧光的激光束透过激发针孔被分光器反射,通过显微物镜汇聚后入射于待观察的标本内部焦点处。激光激发产生的荧光和少量反射激光一起被物镜重新收集后送往分光器。其中携带图像信息的荧光由于波长较长,直接通过分光器并透过检测针孔到达光电探测器(通常是光电倍增管 PMT),变成电信号后送入计算机。由于分光器的分光作用,残余的激光被分光器阻挡,不会被探测到。由于只有焦平面上的点所发出的光才能通过检测针孔,因此焦平面上的观察目标点呈现亮色,而非观察点则呈黑色背景,反差增加,图像清晰。在成像过程中,检测针孔的位置始终与显微物镜的焦点是一一对应的(共

轭)因而被称为共聚焦显微技术(图 2b) (Laurent et al., 1994; Paddock, 2000)。

光焦点在焦平面逐点逐行移动,将采集到的光信号直接传输到控制电脑,经光电信号转换后,控制软件可以把样品焦平面光信号进行虚拟成像,样品表面光信号强度以灰度表示,也可以渲染上色,对图像信息进行更好的展示和分析。由于在荧光显微镜成像基础上加装了激光扫描装置,利用计算机进行图像处理,使用紫外或可见光激发荧光探针,从而得到细胞或组织内部微细结构的荧光图像,加之去卷积技术可确保获得更好的光学切片 (Dey et al., 2006),分辨率提高了 30%~40%,其光学切片性能使观察微观三维结构成为可能 (Fernández-Suárez and Ting, 2008)。总体来说,激光扫描共聚焦显微镜具有图像采集、荧光信号定性和定位、荧光强度定量测定等基本功能。其中,图像采集是荧光信号定位、定性和定量的基础和前提。与其他光学成像技术相比,CLSM 具有很多优



(a) <http://mooc.chaoxing.com/course/89445934.html?edit=false&knowledgeId=89446054&module2;>  
 (b) <http://www.hengqiao.net/fwshow.aspx?NewsId=30>

图2 激光扫描共聚焦显微镜系统组成 (a)、基本原理 (b) 和常用的激光扫描共聚焦显微镜系统 (c)  
 Fig.2 The components (a) and basic principles (b) of the laser scanning confocal microscope system and the commonly used laser scanning confocal microscope systems (c)

势: 无损伤扫描保持样品的完整性、采集多重波段荧光、实现多种荧光信号的共定位分析、图像质量较高、操作控制灵活; 定性和定位荧光物质、定量测定荧光信号等(图2b)(Pawley, 2006)。该技术被广泛用于荧光定量测量、共焦图象分析、三维图象重建、活细胞动力学参数监测和胞间通讯研究等方面, 是生命科学、地球科学、环境科学等领域新一代强有力的研究工具。

### 1.3 成像模式

基本成像模式可分为平面成像、3D 成像、动态

监测、反射和透射成像、光谱成像, 它们在其他高级成像模式的基础。多种基本成像模式联用可实现多通道平面成像、多通道 3D 成像和多通道光谱扫描等。

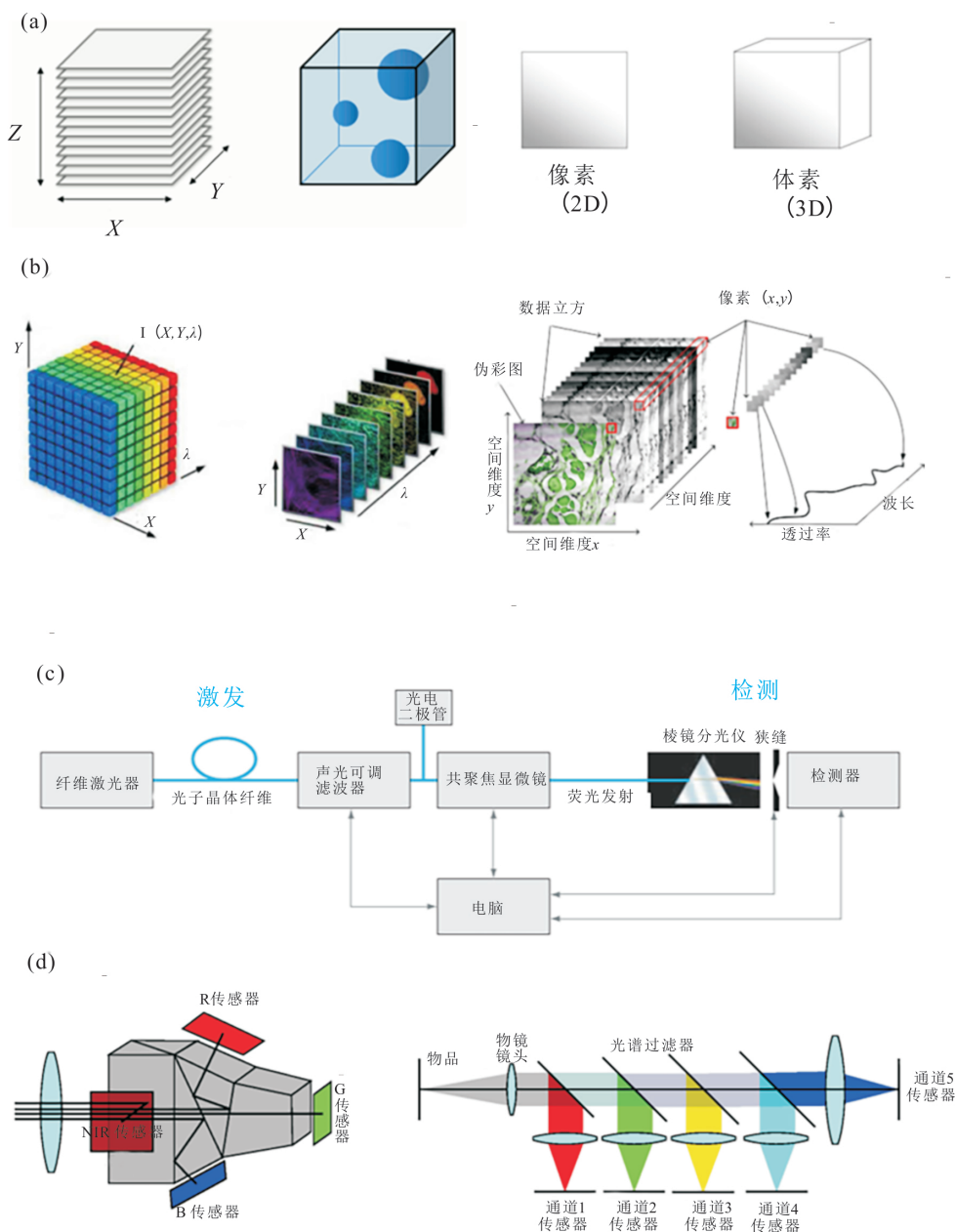
1.3.1 3D 成像 这是最常用的成像模式之一, 其本质是平面成像的累积和图像的 3D 重构 (Carlsson et al., 1985)。逐个焦平面成像形成的平面图像经过软件的重构, 可以实现样品的立体图像展示 (Anderson et al., 1999)。平面图像是由焦点在焦平面逐点逐行进行点扫描获取的信号转换成像素组成



的,每个像素代表了一定的物理尺寸。如果扫描范围是  $50\ \mu\text{m}$ , 图像分辨像素是  $512 \times 512$ , 那么一个像素就代表了  $0.1\ \mu\text{m}$  的物理尺寸。图像的分辨率取决于单位像素代表的物理尺寸,也就是给定的扫描范围,扫描的频率越高,像素越大,图像的分辨率越高。但对于可见光区分析,像素一般设定不超过光学显微镜的极限  $0.2\ \mu\text{m}$ 。体素是 3D 图像构成的基本单位,是相邻像素构成的基本单元。同样,3D 图像的分辨率取决于单位体素代表的物理体积,给定

的扫描体积,扫描的频率越高,体素越大,图像的分辨率越高(图 3a) (Pawley, 2006)。

3D 观察和展示技术可用于实时 3D 细胞示踪 (Rabut and Ellenberg, 2004)、生物膜结构 (Li et al., 2016)、胶原基质量化和重建 (Wu et al., 2003)、3D 活细胞定量成像 (Yu et al., 2011b)、土壤微生物过程 3D 空间成像 (Downie et al., 2014)、多标记多通道三维分子成像 (Maruo et al., 2014) 等,并通过计算机断层模拟和 3D 分析获得精准定



(b) 据 Garini 等(2006); (c) 据 Hiraoka 等(2002)

图 3 激光扫描共聚焦显微镜 3D 成像原理、像素和体素概念(a), 光谱成像原理(b), 光谱成像的系统组成(c) 和多通道成像基本原理(d)

Fig.3 3D imaging principle, pixel and voxel concept of laser scanning confocal microscope (a), spectral imaging principle (b), components of the spectral imaging system (c), and basic principle of the multi-channel imaging system (d)

量测量(Kamburoğlu et al., 2008)。

1.3.2 光谱成像 这是通过成像光谱仪记录被检验物体在一定光谱范围内密集均匀分布的多个窄波段单色光的反射光亮度分布或荧光亮度分布,形成由许多单色光影像构成的光谱影像集。光谱成像记录的光谱影像集包含了检材物体在多幅等间隔波长位置的窄波段单色光亮度分布影像,因此也被称为多光谱成像或超光谱成像。由于这些光谱亮度曲线能够在一定程度上反映被检验物体上物质的化学成分,因此光谱成像又被称为化学成像(图3b)(Tearney et al., 1998)。

目前,多数激光扫描共聚焦显微镜系统整合了显微光谱成像系统,硬件上不仅包括共聚焦成像部分,还整合了光谱探测部分(包括准直透镜、分光棱镜、聚焦透镜、移动狭缝1、移动狭缝2、光电倍增管PMT)(图3c)(Hiraoka et al., 2002)。

激光扫描共聚焦显微镜整合光学光栅可获取高光谱分辨率的荧光图像,这对于监测荧光分子的光谱变化和发射光谱严重重叠的荧光标记有很大帮助(Haraguchi et al., 2002; Zimmermann, 2005)。技术发展和革新使得高速扫描高分辨率的共聚焦显微镜技术成为现实,并用于科学研究(Boudoux et al., 2005; Sinclair et al., 2006; Megías et al., 2009),3D光谱成像也已成为可能(Liu et al., 2002),特别是在生命科学中的应用(Hiraoka et al., 2002; Zimmermann et al., 2003)。

1.3.3 多通道成像 基于多荧光化学标记的多通道激光扫描共聚焦显微镜技术是生物学和显微镜学发展的基本趋势(Zhang et al., 2013b)。多光谱成像和线性分解联用为三维激光扫描共聚焦荧光显微镜分析技术提供了新的维度(Studer et al., 2012)。该技术最早出现于20世纪90年代初(Nudelman and Ouimette, 1992),目前已发展成熟,新兴技术超光谱分析改进了多标记成像检测的质量(Haaland et al., 2009)。通过光谱成像中的分波段信号采集,实现每种波段代表特定的化学组成,实现在同一个三维空间不同组分的图像和光谱分析,从而提供各组分之间在时空分布上的相互关系。通道数量一般取决于目标研究的组分,可获得专一灵敏荧光标记、激发光谱线数量、检测器数量和灵敏度等。通常是先对物体的每个平面、每个设定通道的信号依顺序采集,再逐层对物体进行扫描,最后通过3D重构实现三维组分分析,提供最直观的实验数据和证据(图3d)。

荧光蛋白双标记激光扫描共聚焦显微镜可以

原位非破坏观察生物膜的基因表达(Cowan et al., 2000),甚至质粒的原位转移(Nancharaiiah et al., 2003)。多通道成像分析还被用于确定细菌及其呼吸活性(Ogawa et al., 2005)和生物聚集体EPS的分布(Chen et al., 2007a)等研究。多通道荧光标记技术是实现共定位分析的前提和基础(Scriven et al., 2008),目前最多可实现5个荧光蛋白(Malide et al., 2014)和核酸、蛋白、多种多糖、脂类6种成分(Chen et al., 2006)的多通道激光扫描共聚焦显微镜成像分析,为关联组分和分子的共定位分析奠定了坚实的技术基础。多标记多通道激光扫描共聚焦显微镜已用于脑科学和神经突触的分子共定位分析(Wouterlood, 2014),以及生物膜中细胞、多糖和蛋白的原位观察(Yuan et al., 2015)。为了获得最佳的多标记多通道成像效果,选择荧光探针并兼顾显微镜配制(Lichtman and Conchello, 2005),最大限度避免光谱重叠、荧光基团过饱和、检测器的过饱和、样品采集过高或过低等技术问题(Brown, 2007),以及清除背景噪音(Zimmermann et al., 2014)等方面进行综合考虑和优化(图3d)。

上述技术目前已广泛用于生物学研究(Adams et al., 2003)。同时遗传分子标记和化学荧光标记的飞速发展又推进了多通道成像分析技术的发展和完善(Prow et al., 2004)。

#### 1.4 常见的激光扫描共聚焦显微镜系统

目前,共聚焦有四大厂商:蔡司(Zeiss,德国)、莱卡(Leica,德国)、尼康(Nikon,日本)和奥林巴斯(Olympus,日本)(图2c)。常见的激光扫描共聚焦显微镜系统有Leica TCS SP8 X和TCS SPE, Zeiss LSM 800和LSM 880, Olympus FV3000和FV1200, Nikon AZ-C2+和CSU-Series等。目前,激光扫描共聚焦显微镜系统以提高实验灵敏度、分辨率和速度、避免光毒性或漂白现象、提高实验的重复性、大样本高质量成像为目标。通过一次性收集所有荧光信号,并行采集检测多个荧光标记物,并配备更多数量的共聚焦探测器,利用并行光谱采集和高速GPU去卷积的独特组合,提高图像质量。以更高的灵敏度检测荧光从而减少光毒性,采用灵活高效的声光分光器AOBS,可对光谱接近的染料进行成像,效率提高30%,素来以能够高灵敏度、高速度捕捉活细胞的动态,可以自由选择激发激光线和发射光谱带为发展趋势。

## 2 荧光标记技术

化学荧光探针是生物显微成像分析的基础和

工具(Johnsson and Johnsson, 2007),在标记生化和细胞生物学过程中起着十分重要的作用(Lavis et al., 2006; Liu et al., 2013a),荧光属于化学生物学开创性基础研究(Lavis and Raines, 2008)。如何选择适宜的标记技术,特别是观察、示踪、分析细胞关键蛋白需要综合考虑标记分子和被标记分子的生物化学特性(Marks and Nolan, 2006)。

## 2.1 发展历程和现状

过去20年,金属荧光探针有了长足发展,被广泛用于生命科学研究(Que et al., 2008; Quang and Kim, 2010; Ueno and Nagano, 2011)。与荧光量子点相比,荧光探针容易受所处微环境的影响,相对稳定性低(Resch-Genger et al., 2008; Xiong et al., 2014)。目前,荧光探针的开发倾向于荧光探针库的建立和筛选等高通量方法(Kang et al., 2011; Vendrell et al., 2012; Yuan et al., 2013b);化学分子库策略也被用于荧光探针的开发(Kang et al., 2011; Lee et al., 2011)。化学荧光探针的成像分析是荧光化学的活跃领域(Schäferling, 2012)。而发展多功能荧光标记同时实现对pH、氧气和温度等的检测可能是荧光探针发展的另一个趋势(Stich et al., 2009; Schäferling, 2012)。早期荧光标记技术主要用于细胞信号传导研究和细胞流式技术分析,后来化学荧光探针用于活细胞成像分析、探测氧化还原化学势(Tratnyek et al., 2001)、细菌成像(White et al., 2012)和细菌活性分析(图1b)。尽管我们对于部分荧光探针的光谱特性(Valm et al., 2016)、荧光通量、化学性质(Grimm et al., 2013)以及详细化学合成途径(Nguyen and Francis, 2003; Wysocki et al., 2011)都较熟悉,但设计和创造新的适合生物学需求的荧光探针一直是荧光化学研究者追寻和努力的方向(Zhang et al., 2002; Kikuchi, 2010)。

## 2.2 原理和种类

2.2.1 原理 荧光分子探针设计基本原理和策略是(Vendrell et al., 2012)在了解荧光基团光物理过程和特性的基础上(Stennett et al., 2014)通过添加或置换识别位点改变分子对目标分子的专一识别性和灵敏度(Wu et al., 2012)。荧光探针识别机制涉及不同的化学机制(Qian et al., 2010),包括光诱导分子内电荷转移(Sauer, 2003)、分子共振能量转移(Thivierge et al., 2011)、氧化还原电势反应(Lou et al., 2015)等化学基本过程(图4a)。

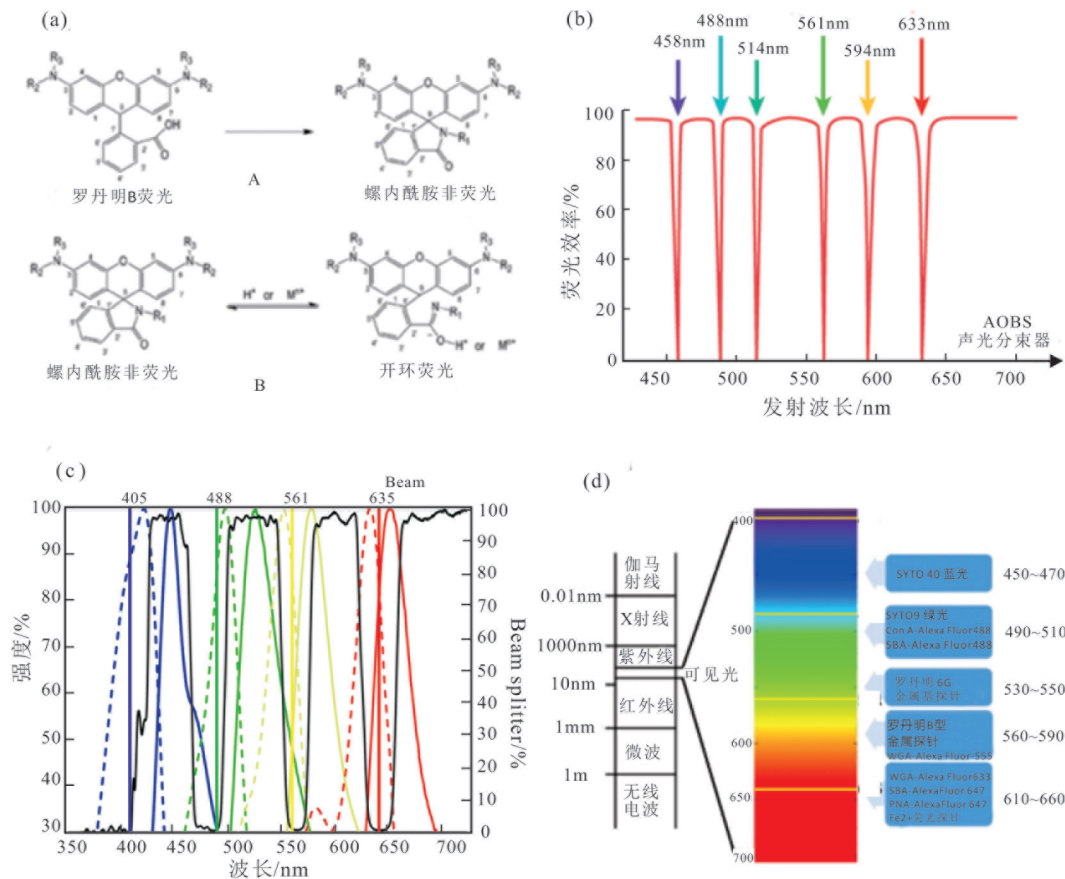
### 2.2.2 主要种类

(1) 金属离子: 从20世纪末第一个金属荧光探针报道开始(Czarnik, 1998; Carter et al., 2014),人

们对不同金属荧光探针的开发从未停止。同时,金属生物学研究对荧光探针合成也提出了新的要求: 更适合金属细胞成像分析(Domaille et al., 2008),并具有可控制的荧光分子开关(Xu et al., 2010)。基于罗丹明衍生物螺环分子开关控制的金属荧光探针在过去20年得到了飞速发展,目前已有上千个不同金属荧光探针的报道,并陆续用于和生物密切相关金属离子的显微分析,特别是在钠、钾、锌、铁、铜、锰、镍、钴等生物必需金属以及铅、镉、汞、铬、金、银、铂等有害金属等探针开发和生物成像研究方面(表1)(Kikuchi et al., 2004; Terai and Nagano, 2008; Beija et al., 2009; Tomat and Lippard, 2010; Zhang et al., 2011a; Kim et al., 2012; Sun et al., 2012; Yang et al., 2013; Carter et al., 2014)。另外,在特殊离子如单价铜(Fahrni, 2013)、适于双光子显微镜的金属荧光(Kim and Cho, 2011)、近红光荧光探针(Guo et al., 2014)方面都时有报道。

(2) 生物分子: 各种核酸、蛋白、脂类和多糖荧光染料都已实现商品化生产和规范化应用(表2)。在小分子荧光核酸探针方面,近几年也有进展(Zhou et al., 2011; Dutta et al., 2012)。除了采用小分子荧光探针对蛋白和酶分子进行化学标记外(Gonçalves, 2009; Lang and Chin, 2013)遗传编码的各种荧光蛋白作为报告基因也被广泛用于生物学蛋白和酶分子的荧光标记和定位观察(Shaner et al., 2005; Drepper et al., 2007; Lagendijk et al., 2010)。而脂类荧光探针也被用于细胞之类标记和显微观察(Trevors, 2003)(表2)。

(3) pH: pH荧光探针早在20世纪80年代就开始用于细胞内pH的成像分析(Slavík, 1983),20世纪90年代有一定发展,但直到最近才用于微生物膜微环境pH的分析(Hunter and Beveridge, 2005)、定量 $p_{CO_2}$ 成像分析(Schutting et al., 2014)和癌细胞的目标分子成像分析(Urano et al., 2009)。通过 $CO_2$ 生产率作为生物膜代谢的指标(Bester et al., 2010)。氟硼二吡咯(Boens et al., 2012)、罗丹明及其衍生物(Chen et al., 2011)、荧光素及其衍生物(Ge and Chen, 2008)都可用于pH荧光探针设计和合成(表3)。甚至出现了双光子激发的pH荧光探针(Kermis et al., 2002)。这类探针的发展和特性,特别是用于细胞内pH检测方面的,都有全面系统的总结和归纳(Han and Burgess, 2010; Li et al., 2014b; Yin et al., 2015)。而超高分辨率显微镜技术的发展,对pH荧光探针的发展提出了新的要求



(a) (c) 引自 Hao 等(2013); (d) 引自 Hao 等(2016)

图4 荧光分子探针设计与工作原理(a) Leica SP8 常用分光器光谱性能(b) Leica SPE 常用分光器光谱性能与四标记优化示意(c) 和多标记实验方案设计(d)

Fig.4 The design and working principle of fluorescent molecular probe (a), performance of spectral separation of Leica SP8 spectrometer (b), performance of spectral separation and four-label optimization of Leica SPE spectrometer (c), and design of multi-label experimental scheme (d)

(Lacivita et al., 2012)。特别是基于多功能多标记的 pH、氧气和温度的同时检测及其生物学应用 (Mothammer et al., 2016; Zou et al., 2017)。

(4) 活性分子: 荧光探针除了可以用于标记金属离子、活性生物分子外, 还被广泛用于活性氧分子、活性氮分子等与生物代谢密切相关的小分子物质的显微成像分析 (Tanaka et al., 2001; Gomes et al., 2005, 2006; Baleizao et al., 2008)。在生物活性气体荧光探针研究方面, 目前已报道的有二氧化碳荧光探针 (Liu et al., 2010; Xu et al., 2013)、一氧化碳荧光探针 (Wang et al., 2012; Yuan et al., 2013a) 和一氧化氮荧光探针 (Kumar et al., 2013)。

此外, 在特殊类型探针开发方面也有些进展, 如荧光温度探针的开发取得了开创性成果 (Wang et al., 2013), 砷荧光探针也时有报道 (Parker et al., 2005; Ezech and Harrop, 2012)。酸性条件稳定的荧光探针 (Brockmann et al., 2010)、多胺荧光探针

(Lodeiro et al., 2010) 有机磷杀虫剂荧光探针 (Obare et al., 2010)、过氧亚硝酸盐荧光探针 (Xu et al., 2011a) 及其显微应用也见有报道。

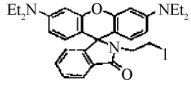
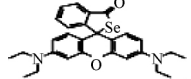
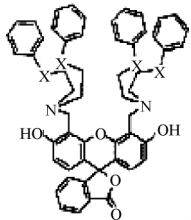
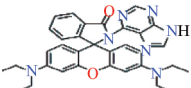
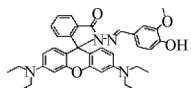
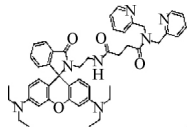
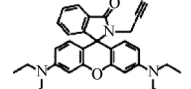
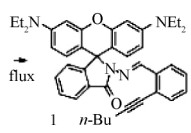
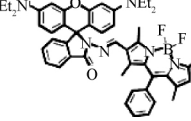
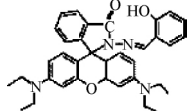
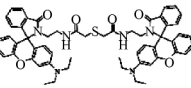
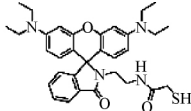
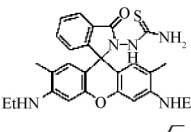
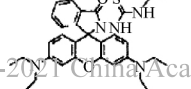
(5) 限制: 由于单分子荧光对其所处环境十分敏感, 其荧光闪烁和关闭时间并不遵循固有特定的规律 (Clifford et al., 2007), 这就对共聚焦显微分析中荧光探针的选择、储存、溶液配制、标记和分析的操作规程提出了严格的要求 (Cullander, 1999), 而大部分水溶性荧光探针由于和细胞脂双层作用而影响标记效果 (Hughes et al., 2014), 此外荧光探针所处微环境的氧气浓度也会影响其光效率 (Jensen, 2012; Icha et al., 2017)。

### 3 探针选择和方案设计

#### 3.1 探针选择

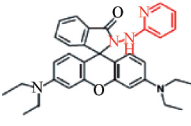
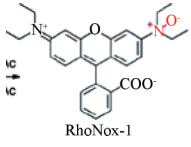
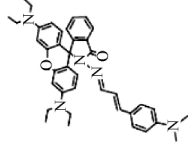
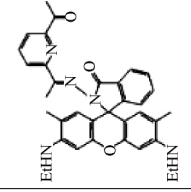
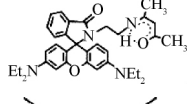
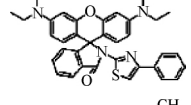
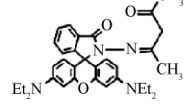
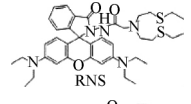
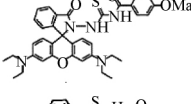
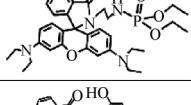
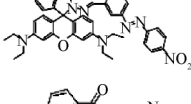
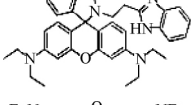
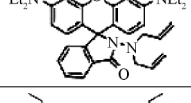
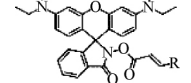
荧光探针的选择需要考虑: ① 化学性质、光谱特性、线性检测范围、灵敏性和专一性等; ② 目标分

表 1 部分金属荧光探针  
Table 1 Some metal fluorescent probes

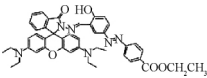
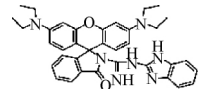
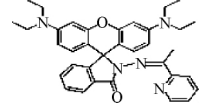
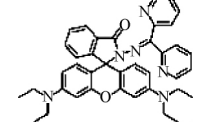
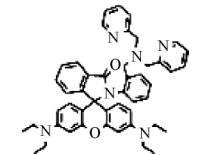
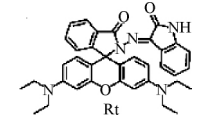
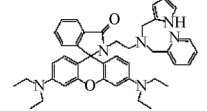
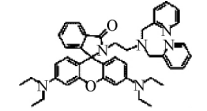
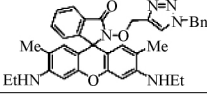
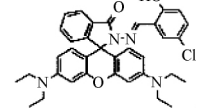
识别金属离子	化学结构式	$E_x$ /nm	$E_m$ /nm	检测极限	SDR/ $\mu$ M	工作溶液	参考文献
Ag <sup>+</sup>		530	584	14×10 <sup>-9</sup>	0.1~5	EtOH	Chatterjee 等(2009)
		520	580	52 nM	0.1~10	H <sub>2</sub> O	Shi 等(2010)
		463	538	4 nM	0~1	EtOH	Liu 等(2014a)
Al <sup>3+</sup>		566	590	0.19 $\mu$ M	0~8	DMSO-H <sub>2</sub> O	Sahana 等(2016)
		520	587	0.14 $\mu$ M	0~100	MeOH-DMSO	Gupta 等(2015)
		560	582	0.196 $\mu$ M	5~16	EtOH-H <sub>2</sub> O	Bao 等(2015b)
Au <sup>3+</sup>		558	579	100×10 <sup>-9</sup>	0.5~4	EtOH-H <sub>2</sub> O	Jou 等(2009)
		500	580	0.6×10 <sup>-6</sup>	1~100	CH <sub>3</sub> CN-HEPES	Karakuş 等(2013)
		470 525	506 585	10 65 nM	0~0.3	CH <sub>3</sub> CN-HEPES	Emrullahoğlu 等(2013)
Cr <sup>3+</sup>		520	591	0.0015 $\mu$ M	0.01~0.3	H <sub>2</sub> O	Zheng 等(2009)
		556	580	0.378 $\mu$ M	0~300	—	Bao 等(2015a)
		520	580	1×10 <sup>-6</sup>	0~10	MeOH-H <sub>2</sub> O	Li 等(2014a)
Cu <sup>2+</sup>		480	554	0.002 $\mu$ M	0~0.005	CH <sub>3</sub> CN	Huang 等(2011)
		510	580	10×10 <sup>-9</sup>	4.5~160×10 <sup>-9</sup>	CH <sub>3</sub> CN-HEPES	Yu 等(2008)



续表1

识别金属离子	化学结构式	$E_x$ /nm	$E_m$ /nm	检测极限	SDR/ $\mu$ M	工作溶液	参考文献
Cu <sup>2+</sup>		540	575	21 nM	0.5~3	EtOH <sup>①</sup>	Yang 等(2011b)
	 RhoNox-1	540	575	0.2 $\mu$ M	—	HEPES	Hirayama 等(2013)
Fe <sup>2+</sup>		380	470~582	60 nM	0~20	THF	Kumar 等(2011)
		510	571	—	2~24	PBS	Hou 等(2013)
Fe <sup>3+</sup>		561	583	0.11 $\mu$ M	1~18 18~100	EtOH	Dong 等(2010)
		558	580	5 $\mu$ M	5~20	MeOH	She 等(2012)
		570	593	4 nM	0.5~50	EtOH	Zhang 等(2011b)
		520	586	—	0~50	HEPES	Chen 等(2013)
Hg <sup>2+</sup>		565	590	1.7 nM	0.1~1	DMF-HEPES	Liu 等(2013b)
		550	590	0.2 $\times$ 10 <sup>-6</sup>	0~10	H <sub>2</sub> O	Zhang 等(2013a)
		561	579	0.45 $\mu$ M	0~100	EtOH-H <sub>2</sub> O	Mahapatra 等(2015)
Pd <sup>2+</sup>		525	569	21 nM	0~60	EtOH-H <sub>2</sub> O	Chen 等(2016)
		530	580	0.185 $\mu$ M	0~1 $\times$ 10 <sup>-6</sup>	EtOH-H <sub>2</sub> O	Li 等(2010)
Sn <sup>2+</sup>		520	582	0.9 $\mu$ M	1~16	EtOH-HEPES	Cheng 等(2015)

续表1

识别金属离子	化学结构式	$E_x$ /nm	$E_m$ /nm	检测极限	SDR/ $\mu$ M	工作溶液	参考文献
Sn <sup>2+</sup>		563	582	7.1 $\mu$ M	0~400	EtOH-H <sub>2</sub> O	Mahapatra 等(2014)
		540	581	0.03 $\mu$ M	0~50	PBS	Yang 等(2017)
Zn <sup>2+</sup>		535	578	29 nM	0~50	HEPES	Ozdemir(2016)
		530	581	—	0.2~50	EtOH-H <sub>2</sub> O	Xu 等(2011b)
		550	595	—	0~1.8 mm	PIPES	Du 和 Lippard(2010)
Cd <sup>2+</sup>		563	582	—	1~20	HEPES	Xu 等(2012)
Co <sup>2+</sup>		500	582	4.3 nM	1~10	THF-H <sub>2</sub> O	Biswal 等(2016)
Pb <sup>2+</sup>		510	575	—	—	CH <sub>3</sub> CN	Kwon 等(2005)
Pt <sup>2+</sup>		500	562	0.1 $\mu$ M	0.1~5	DMSO	Kim 等(2010)
V <sup>4+</sup>		530	583	0.1 $\mu$ M	0.1~10	MeOH-HEPES	Huo 等(2010)

注: EtOH 为乙醇; H<sub>2</sub>O 为水; DMSO 为二甲基亚砜; MeOH 为甲醇; CH<sub>3</sub>CN 为乙腈; HEPES 为 4-(2-羟乙基)-1-哌嗪乙烷磺酸; THF 为四氢呋喃; PBS 为磷酸盐缓冲液; DMF 为二甲基甲酰胺; PIPES 为哌嗪-1,4-二乙磺酸; “—”未知;  $E_x$  为激发光峰值;  $E_m$  为发射光峰值; SDR 为检测范围。

子/离子的化学性质、分布位点、浓度范围以及化学价态、所处的生物化学/地球化学梯度、pH 以及氧化还原电位、与之作用的化学基团性质、电荷等; ③样品的透光率和吸光率、有无自发荧光、与荧光探针相互作用的稳定性等; ④激光扫描共聚焦显微镜的激光类型种类以及数量、激发效率、分光器光谱性能、检测器检测范围和灵敏度(图 4b)。总之, 荧光探针的特性要尽可能的在待检测样品系统中保持化学性能和光学性质稳定, 检测范围与待检测目标的浓度范围一致, 检测过程中与使用的激光扫描共

聚焦显微镜系统硬件参数相互匹配兼容, 多标记成像分析中要与其他荧光探针和染料光谱尽量避免相互重叠(Hao et al., 2013)。

理想的荧光标记对于激光扫描共聚焦显微镜分析至关重要, 其中最基本的是荧光探针在实验检测条件下保持高度的灵敏性和专一性。以荧光金属探针的选择为例, 荧光探针选择需要从以下几个方面开始考虑(Hao et al., 2013)。

(1) 以地球微生物和环境微生物样品中的金属离子为例, 首先要明确金属离子是分布于细胞内还

表 2 生物大分子核酸、蛋白、脂类和多糖残基荧光染料和标记物

Table 2 Biological macromolecule nucleic acid, protein, lipid and polysaccharide residue fluorescent dyes and markers

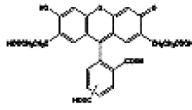
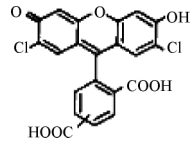
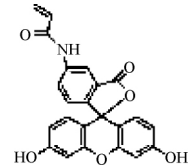
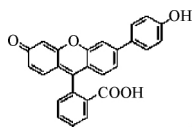
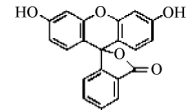
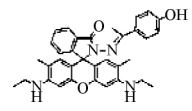
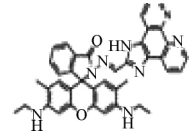
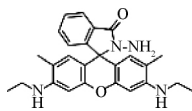
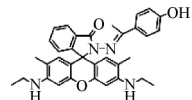
荧光探针	$L_w$ / nm	SDR / nm	$E_x$ / nm	$E_m$ / nm	识别目标分子
核酸荧光染料					
SYTO <sup>®</sup> 40 blue	405	415~475	419	445	细胞总核酸
SYTO <sup>®</sup> 9 green	488	496~560	483	503	细胞总核酸
SYTO <sup>®</sup> 84 orange	561	570~620	567	582	细胞总核酸
SYTO <sup>®</sup> 62 red	635	640~700	649	680	细胞总核酸
SYTOX <sup>®</sup> Blue	405	415~485	444	480	细胞核 核酸
SYTOX <sup>®</sup> Green	488	496~560	504	523	细胞核 核酸
SYTOX <sup>®</sup> Orange	561	570~620	547	570	细胞核 核酸
SYTOX <sup>®</sup> Red	635	640~700	640	658	细胞核 核酸
DAPI	—	—	358	461	—
蛋白荧光染料					
SYPRO <sup>®</sup> Orange	488	496~560	470	570	细胞总蛋白
SYPRO <sup>®</sup> Red	561	570~620	550	630	细胞总蛋白
SYPRO <sup>®</sup> Tangerine	488	570~620	490	640	细胞总蛋白
NanoOrange	488	496~560	470	570	细胞总蛋白
细胞脂类荧光染料					
DiO <sup>+</sup> ; DiOC18(3)	484	501	—	—	—
DiI <sup>+</sup> ; DiIC18(3)	549	565	—	—	—
DiD <sup>+</sup> oil; DiIC18(5)	644	665	—	—	—
DiR <sup>+</sup> ; DiIC18(7)	750	780	—	—	细胞膜和脂类
Lectin-Alexa Fluor 缀合体(多糖残基荧光标记)					
Concanavalin A, Alexa Fluor <sup>®</sup> 488	488	496~560	495	519	$\alpha$ -甘露聚糖基 $\alpha$ -吡喃葡萄糖基残基
Concanavalin A, Alexa Fluor <sup>®</sup> 633	635	640~700	632	647	$\alpha$ -甘露聚糖基 $\alpha$ -吡喃葡萄糖基残基
Wheat Germ Agglutinin, Alexa Fluor <sup>®</sup> 488	488	496~560	495	519	N-乙酰氨基葡萄糖和 N-乙酰神经氨酸残基
Wheat Germ Agglutinin, Alexa Fluor <sup>®</sup> 555	561	570~620	555	565	N-乙酰氨基葡萄糖和 N-乙酰神经氨酸残基
Wheat Germ Agglutinin, Alexa Fluor <sup>®</sup> 633	635	640~700	632	647	N-乙酰氨基葡萄糖和 N-乙酰神经氨酸残基
Wheat Germ Agglutinin, Alexa Fluor <sup>®</sup> 680	635	640~700	679	702	N-乙酰氨基葡萄糖和 N-乙酰神经氨酸残基
Lectin PNA From Arachis hypogaea (peanut), Alexa Fluor <sup>®</sup> 488	488	496~560	495	519	末端 $\beta$ -半乳糖
Lectin PNA From Arachis hypogaea (peanut), Alexa Fluor <sup>®</sup> 568	561	570~620	579	603	末端 $\beta$ -半乳糖
Lectin PNA From Arachis hypogaea (peanut), Alexa Fluor <sup>®</sup> 647	635	640~700	650	668	末端 $\beta$ -半乳糖
Lectin SBA From Glycine max (soybean), Alexa Fluor <sup>®</sup> 488	488	496~560	495	519	末端 $\alpha$ -和 $\beta$ -N-乙酰半乳糖胺和吡喃半乳糖基残基
Lectin SBA From Glycine max (soybean), Alexa Fluor <sup>®</sup> 594	561	570~630	590	617	末端 $\alpha$ -和 $\beta$ -N-乙酰半乳糖胺和吡喃半乳糖基残基
Lectin SBA From Glycine max (soybean), Alexa Fluor <sup>®</sup> 647	635	640~700	650	668	末端 $\alpha$ -和 $\beta$ -N-乙酰半乳糖胺和吡喃半乳糖基残基
Lectin HPA From Helix pomatia (edible snail), Alexa Fluor <sup>®</sup> 488	488	496~560	495	519	$\alpha$ -N-乙酰半乳糖胺残基
Lectin HPA From Helix pomatia (edible snail), Alexa Fluor <sup>®</sup> 647	635	640~700	650	668	$\alpha$ -N-乙酰半乳糖胺残基
Lectin PHA-L From Phaseolus vulgaris (red kidney bean), Alexa Fluor <sup>®</sup> 488	488	496~560	495	519	$\alpha$ -N-乙酰半乳糖胺残基
Lectin GS-II From Griffonia simplicifolia, Alexa Fluor <sup>®</sup> 488	488	496~560	495	519	末端非还原性 $\alpha$ -或 $\beta$ -连接的 N-乙酰基-D-葡萄糖胺
Lectin GS-II From Griffonia simplicifolia, Alexa Fluor <sup>®</sup> 647	635	640~700	650	668	末端非还原性 $\alpha$ -或 $\beta$ -连接的 N-乙酰基-D-葡萄糖胺

续表2

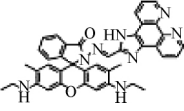
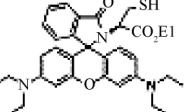
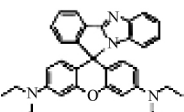
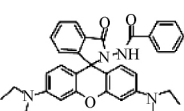
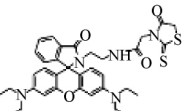
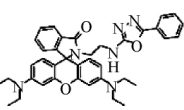
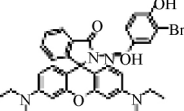
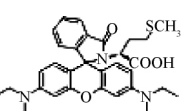
荧光探针			$L_w$ / nm	SDR / nm	$E_x$ / nm	$E_m$ / nm	识别目标分子
Isolectin simplicifolia	GS-IB4 , Alexa Fluor®	From Griffonia	488	496~560	495	519	A 亚基偏爱 N-乙酰基-D-半乳糖胺端基, 而 B 亚基对末端 $\alpha$ -D-半乳糖基残基具有选择性 terminal a-D-galactosyl residues
Isolectin simplicifolia	GS-IB4 , Alexa Fluor®	From Griffonia	561	570~620	579	603	A 亚基偏爱 N-乙酰基-D-半乳糖胺端基, 而 B 亚基对末端 $\alpha$ -D-半乳糖基残基具有选择性 terminal a-D-galactosyl
Isolectin simplicifolia	GS-IB4 , Alexa Fluor®	From Griffonia	635	640~700	650	668	A 亚基偏爱 N-乙酰基-D-半乳糖胺端基, 而 B 亚基对末端 $\alpha$ -D-半乳糖基残基具有选择性 terminal a-D-galactosyl

注:  $L_w$  为激发激光波长; SDR 为检测光谱范围;  $E_x$  为激发光峰值;  $E_m$  为发射光峰值。总结和修改自: <https://www.thermofisher.com/ch/zh/home/references/molecular-probes-the-handbook.html>

表 3 部分荧光 pH 探针  
Table 3 Some fluorescent pH probes

化学结构式	$E_x$ / nm	$E_m$ / nm	SDR	工作溶液	参考文献
	475	540	—	—	Hille 等(2008)
	440	500	3~5	HEPES	Nedergaard 等(1990)
	488	525	6.25~7.25	PBS	Sun 等(2006)
	450	550	7~10	—	Unciti-Broceta 等(2009)
	—	—	7~8	—	Ferrari 等(2013)
	510	560	1~4	—	Liu 等(2014b)
	520	556	1~3.5	MeOH: HCl	Ma 等(2015)
	500	550	4~6	DMF	Zhang 等(2011c)
	510	560	1~4	THF/Tris-HCl	Liu 等(2014b)

续表3

化学结构式	$E_x$ / nm	$E_m$ / nm	SDR	工作溶液	参考文献
	520	555	1~4	MeOH: HCl; MeOH; BRB	Ma 等( 2015)
	563	584	4~5.3	—	Lv 等( 2013a)
	565	600	5~6.5	PBS	Xue 等( 2014)
	525	585	4.5~5	EtOH	Zhang 等( 2009)
	561	585	4.2~5.2	EtOH-BRB	Zhao 等( 2014)
	565	603	4.7~5.7	EtOH	Lv 等( 2013b)
	560	577	1.75~4.0	EtOH-BRB	Yang 等( 2016)
	559	585	3.5~9.7	EtOH: H <sub>2</sub> O	Yu 等( 2016)

注: HEPES 为 4-(2-羟乙基)-1-哌嗪乙烷磺酸; PBS 为磷酸盐缓冲液; MeOH 为甲醇; DMF 为二甲基甲酰胺; THF 为四氢呋喃; BRB 为伯瑞坦-罗比森缓冲溶液; EtOH 为乙醇; H<sub>2</sub>O 为水; “—”表示未知;  $E_x$  为激发光峰值;  $E_m$  为发射光峰值; SDR 为检测范围。

是细胞外,对于大多数生命必须金属离子,作为蛋白酶的活性位点,其浓度范围多在纳摩尔水平(Posth et al., 2010)。所以,即便是细胞外重金属离子浓度达到或高于几个数量级的细胞内对应重金属离子浓度,但细胞始终可通过一定的分子生物保护机制保持细胞内离子维持在较低水平。

(2) 实验条件下金属离子所处的 pH 和氧化还原微环境。微生物形成微环境地球化学梯度有利于提高营养吸收和代谢产能效率,这就造成细胞内外 pH、离子强度和氧化还原电势的差异,而 pH 对金属可溶性的影响很难与吸附位点和荧光探针的质子化区分开来。因此,实验条件下保证荧光探针检测范围涵盖目标金属离子的浓度水平是至关重要的。pH 除了能够降低荧光探针的选择性,还会影响金属和样品的化学形态(Sauvé et al.,

2000)。此外,样品微环境氧化还原条件也会影响金属离子的化学形态。因此,初步确定氧化还原条件、明确目标金属离子的浓度范围对于激光扫描共聚焦显微镜分析十分重要(Hunter and Beveridge, 2008)。

(3) 样品中金属离子的浓度范围。微生物培养条件下多数生物代谢必须的金属离子浓度范围为 10~800 nM(Posth et al., 2010),但自然环境中则不然,可以从类似水平到几个数量级的差别。荧光金属探针灵敏性有可能不能满足特定样品中金属化学形态的全部要求,因此需要进行严格的平行试验控制。通常情况下,金属离子在微环境趋于通过吸附或络合等作用产生富集,这取决于系统中固相介质的表面特性和功能基团。对于微生物-胞外多糖-矿物聚集系统,一部分金属倾向于与有机质表面



的功能基团结合,而少部分倾向于吸附或共沉淀到生物质矿物晶体内部。

(4) 目标金属离子对荧光金属探针的扰动敏感。荧光金属探针的介入有可能改变目标金属离子的分布、迁移、生物可获得性,从而使其正常的生理代谢。这些潜在的影响取决于探针的溶解性和解离常数,进而决定探针的检测范围和对样品的扰动程度。此外,荧光探针标记也可能影响细胞代谢,从而造成探针本身的不均一分布而影响检测结果。

(5) 探针类型。对于定量和半定量分析,几乎所有基于罗丹明分子的高灵敏高选择性的荧光探针都可用于激光扫描共聚焦显微镜重金属成像分析。对于绝对定量分析,高精度高选择性双发射峰比率型荧光探针更有优势,它可减少荧光背景,避免其他非目标离子的干扰(Tsien and Poenie, 1986)。

所选荧光金属探针需要满足灵敏性和高度选择性以及荧光信号稳定(Wuertz et al., 2000)。特别是针对包含多种不同浓度范围的复杂环境样品,荧光金属探针的选择至关重要,目前商品化的探针主要的缺陷就是缺乏足够的高度选择性。此外,所选探针最好在短时间内有较强的荧光增强效应;最好不要被样品中存在的目标金属离子饱和,并且探针能够在较宽的金属浓度范围具有较好的线性关系;要具有较好的水溶性,较低的细胞代谢毒性,对环境无害;最后还要考虑激光扫描共聚焦显微镜硬件光路系统配置,通常选择可见光区激发和发射的荧光金属探针(Hao et al., 2013)。总之,荧光金属

探针的基本选择规律正如该方法的建立者 Czarnik (1998) 所说“不多不少,满足应用的一切需要”。

基于以上考虑,结合实验室可利用的激光扫描共聚焦显微镜系统配置(表4,图4c)以及所采用的模式铁氧化微生物系统,对2017年前的基于罗丹明及其衍生物的大部分荧光金属探针的化学结构、光谱学特性、检测灵敏性、检测范围、选择性等进行了系统总结和比较,初步选择出16种金属离子、38个高选择性和高灵敏性、激发和发射光谱位于可见光区、荧光信号增强型、在较宽的金属浓度范围具有较好的线性关系、水溶性好、细胞代谢毒性低、对环境无害、与已知的激光扫描共聚焦显微镜系统具有良好兼容性的荧光金属探针,它们大都成功地应用于微生物铁氧化、微生物重金属吸附等成像分析,与样品具有良好的兼容性(Hao et al., 2013, 2016)。

### 3.2 方案设计

多标记最初是用于免疫荧光化学标记,主要用于观察两种不同组分在空间上分布状况和共定位趋势等(Brismar and Ulfhake, 1997; Herbert et al., 1999; Jaiswal et al., 2003; Hoffman, 2005; Marras, 2006; Pluth et al., 2011)。常见的可用于激光扫描共聚焦显微镜分析的荧光标记包括自发荧光、遗传标记荧光蛋白、化学标记荧光(Lukinavičius et al., 2016)。多标记的基本原则是尽可能的避免荧光激发/发射光谱的重叠(Suzuki et al., 1998),兼顾激发效率和分光器的性能(Neher and Neher, 2004);优点是不同激光

表4 实验方案设计

Table 4 Basic principle of experimental design

荧光探针	$L_w$ /nm	SDR /nm	$E_s$ /nm	$E_m$ /nm	目标分子或离子
单金属离子-细胞-多糖标记方案					
SYTO® 9 Green	488	496~560	485	498	细胞总核酸
Rhodamine B based metal probe	561	570~620	560	580	目标金属离子
WGA Conjugates, Alexa Fluor® 633	635	640~700	632	647	N-乙酰氨基葡萄糖和N-乙酰神经氨酸残基
双金属离子-细胞-多糖标记方案					
SYTO® 40 Blue	405	415~475	420	441	细胞总核酸
Rhodamine 6G based metal probe	488	496~560	500	545	目标金属离子
Rhodamine B based metal probe	561	570~620	560	580	目标金属离子
WGA Conjugates, Alexa Fluor® 633	635	640~700	632	647	N-乙酰氨基葡萄糖和N-乙酰神经氨酸残基
三金属离子-细胞标记方案					
SYTO® 40 Blue	405	415~475	420	441	细胞总核酸
Rhodamine 6G based metal probe	488	496~560	500	545	目标金属离子
Rhodamine B based metal probe	561	570~620	560	580	目标金属离子
Fluorescent probes for Fe( II ) 2	561	640~700	569	635	亚铁离子

注: $L_w$ 为激光波长;SDR为光谱检测范围; $E_s$ 为激发光峰值; $E_m$ 为发射光峰值。据Hao等(2013, 2016) http://www.cnki.net

激发,采集不同波段的荧光信号,从而在同一样品观察位点提供多种目标分子的分布信息(Carlsson et al., 1994),进而通过图像分析对两两组分之间的共定位趋势进行统计分析,从空间尺度上对目标分子/离子进行直接观察和分析(Johnson, 2006; Yuan et al., 2015)。本小节以多通道光谱3D成像技术联用为例,介绍微生物铁氧化耦合重金属吸附荧光多标记实验设计(表4,图4d)(Fili and Toseland, 2014; Liu et al., 2017)。

(1) 亚铁离子作为代谢底物和电子供体,无氧中性环境中主要以可溶性形式存在于培养基中,起始浓度在毫摩尔水平,随着微生物铁氧化接近稳定期,最终浓度维持在微摩尔水平;而铁离子在无氧中性溶液中基本可以忽略,其主要存在于细胞周质空间和细胞及胞外多糖表面,浓度在微摩尔水平。因此,对于微生物氧化过程中亚铁离子和铁离子的标记,需要选择灵敏度在亚微摩尔水平、选择性好,符合基本要求的荧光金属探针(Thompson, 2005; Simpson, 2013)。对于亚铁-铁离子双标记分析,采用基于氟硼二吡咯-青兰素-三联吡啶光谱的亚铁荧光探针和基于罗丹明衍生物的铁离子探针联用,已成功用于微生物铁氧化及耦合重金属吸附研究中(表1,表4,图4d)。

(2) 其他重金属(如铜、锌、镍、钴等)作为微生物生长必需元素,其浓度始终维持在10~800 nM范围,远低于理论荧光金属探针的检测灵敏度,因此吸附实验需要补充相应的金属浓度至微摩尔水平。对于非必需有毒金属元素(如汞、铅、镉、铬等),极低的浓度也会导致微生物代谢毒性,吸附实验需要考虑这些金属的半致死浓度,选择合适的起始浓度十分重要。对于亚铁/铁离子-重金属双标记分析,采用基于罗丹明衍生物的亚铁/铁离子探针和基于罗丹明6G的重金属荧光探针联用,已成功用于微生物铁氧化耦合重金属吸附的研究(表1,表4,图4d)。

(3) 微生物细胞是铁氧化的主要执行者,微生物铁氧化显微观察和分析离不开对细胞的观察,细胞荧光标记可通过分子遗传荧光蛋白标记,也可通过核酸和蛋白等荧光染料进行标记(Suzuki et al., 1998; Stephanopoulos and Francis, 2011; Hori and Kikuchi, 2013; Schneider and Hackenberger, 2017)。考虑到分子遗传标记较为耗时,通常采用核酸或者蛋白标记,常用的荧光染料如表2所示。先前的研究采用核酸荧光染料 Syto9 或 Syto40 对细胞核酸标记, Syto 系列表现出和上述荧光金属探针良好的兼容性(表4,图4d)(Chen et al., 2007a)。

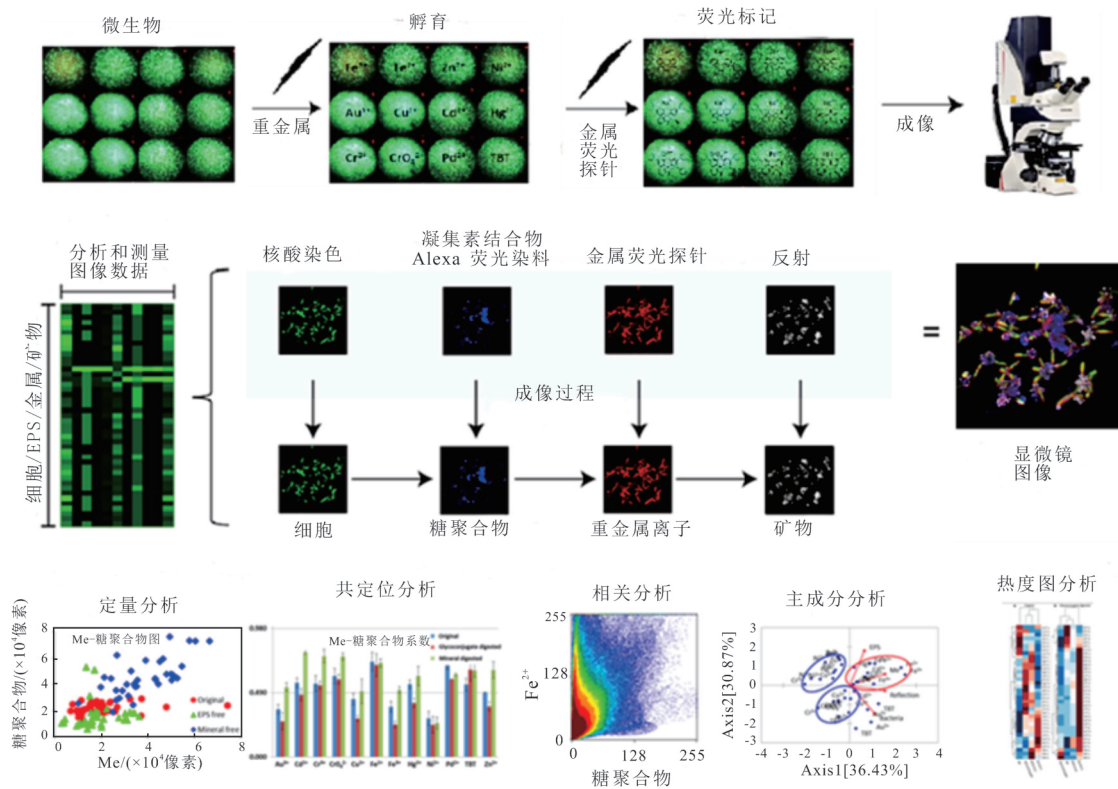
(4) 微生物胞外多糖作为微生物代谢的产物和胞外铁氧化产物的模板,在微生物铁氧化和重金属吸附过程中发挥了重要作用,其主要成分是多糖、蛋白等,传统的对微生物胞外多糖的显微观察主要是利用凝集素识别多糖残基,同时凝集素桥接荧光基团来实现(Chen et al., 2007a; Yu et al., 2011a; Schlafer and Meyer, 2017)。目前常用的凝集素-Alexa 缀合物如表2所示。笔者先前的实验主要采用发射光谱在接近蓝光的凝集素-Alexa 缀合物标记胞外多糖(表4,图4d)。

(5) 考虑到微生物铁氧化系统中关注的对象主要是重金属、铁氧化、微生物细胞及胞外多糖、生物铁矿物,重金属的吸附具有明显的分布异质性,其吸附位点状态可能会受标记的影响,因此先对重金属进行标记(Nosyk et al., 2008)。铁氧化过程主要发生在微生物细胞周围,亚铁/铁离子的分布主要围绕细胞及周围的胞外多糖,在多金属标记实验中可以稍后进行。而微生物细胞作为该系统的始作俑者,始终进行代谢活动,其标记可以和胞外多糖一起进行。实验表明,上述标记顺序有利于最终的激光扫描共聚焦显微镜成像和分析。实验方案和具体操作流程见表4和图5。

## 4 应用

### 4.1 金属-微生物相互作用的原位微观观察

由于金属环境行为和微生物代谢活动相互关系复杂(Warren and Haack, 2001),样品制备期间不可避免的原位信息破坏而干扰了检测结果(Dohnalkova et al., 2011),特别是脱水和临界点干燥或包埋处理通常涉及的溶剂和化学药品,都可改变原位化学成分分布和浓度(Chang and Rittmann, 1986),从而改变金属环境行为和微生物代谢活动的相互关系。定量微区原位分析金属与微生物细胞、胞外多糖和生物质来源矿物的空间关系,确定各组分对重金属环境行为的影响一直是地球微生物学研究的难点,最近原位表征和成像分析生物膜微过程也受到关注(Zhang et al., 2019a, 2019b)。金属离子与微生物细胞、胞外多糖和生物质来源矿物的微观空间关系可以通过激光扫描共聚焦显微镜观察来实现,从而揭示微生物细胞、胞外多糖和生物质来源矿物控制有毒的重金属离子原位微观过程的机制(Hao et al., 2013, 2016; Swanner et al., 2015a, 2015b)。金属荧光探针的出现使激光扫描共聚焦显微镜原位分析金属分布和微观过程成为现实(McRae et al., 2009),实现了胞



据 Hao 等 (2013, 2016) 修改

图 5 多标记激光扫描共聚焦显微镜分析实验操作流程

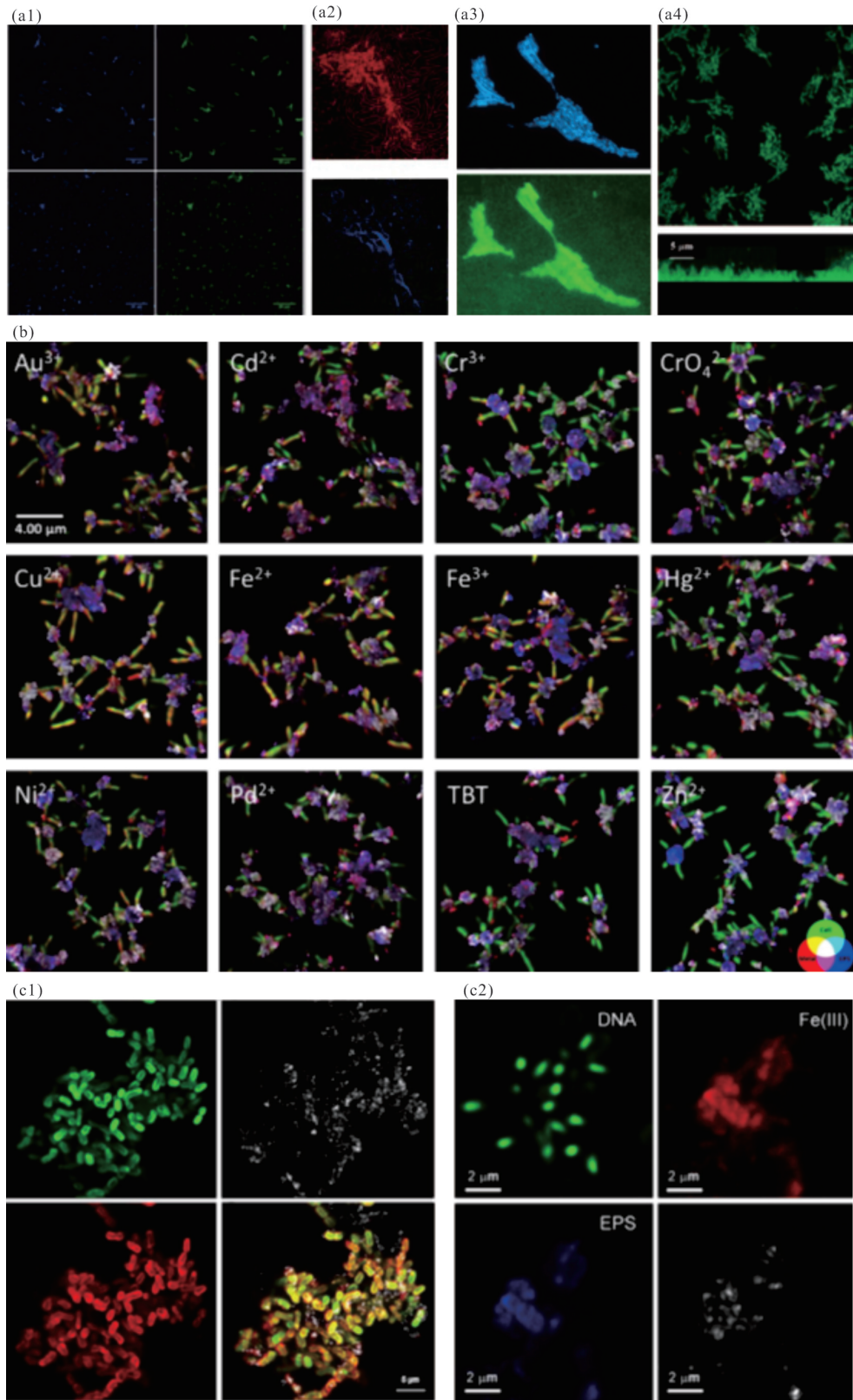
Fig.5 Workflow for the multi-marker laser scanning confocal microscope analysis

内铁离子 (Petrat et al., 2000) 和胞外铜离子 (Ackerman et al., 2017) 微观成像分析。微生物膜锌的空间分布 (Hu et al., 2005)、铜的空间分布 (Hu et al., 2007)、铁的分布和定位 (Julien et al., 2014)、镍的定位和吸附特征 (Lawrence et al., 2019) 也得到了比较精细的显微分析结果, 实现了最接近原始状态下生物膜金属的空间分布成像分析, 揭示了重金属在不同生物膜中不均一性分布特征 (McLean et al., 2008; Hao et al., 2013, 2016; Swanner et al., 2015a, 2015b), 最终实现了定量分析细菌对重金属吸附的三维立体微观作用特征 (Johnson et al., 2018) (图 6)。但是, 不足之处是部分商品化的金属荧光探针选择性相对较差, 不能有效专一区分目标重金属离子 (Wuertz et al., 2000; Ueshima et al., 2008; Shumi et al., 2009)。

#### 4.2 微生物膜微结构组成和微环境

定量化微区原位生物化学组成分析是确定微生物细胞、胞外多糖和生物物质来源矿物各组分对重金属环境行为影响, 原位微区表征和分析是生物膜微过程的关键 (Zhang et al., 2019a, 2019b)。早期主要研究微生物微观结构 (Chen et al., 2006) 和物质组成 (Halan et al., 2012) 等方面的分布和可视化

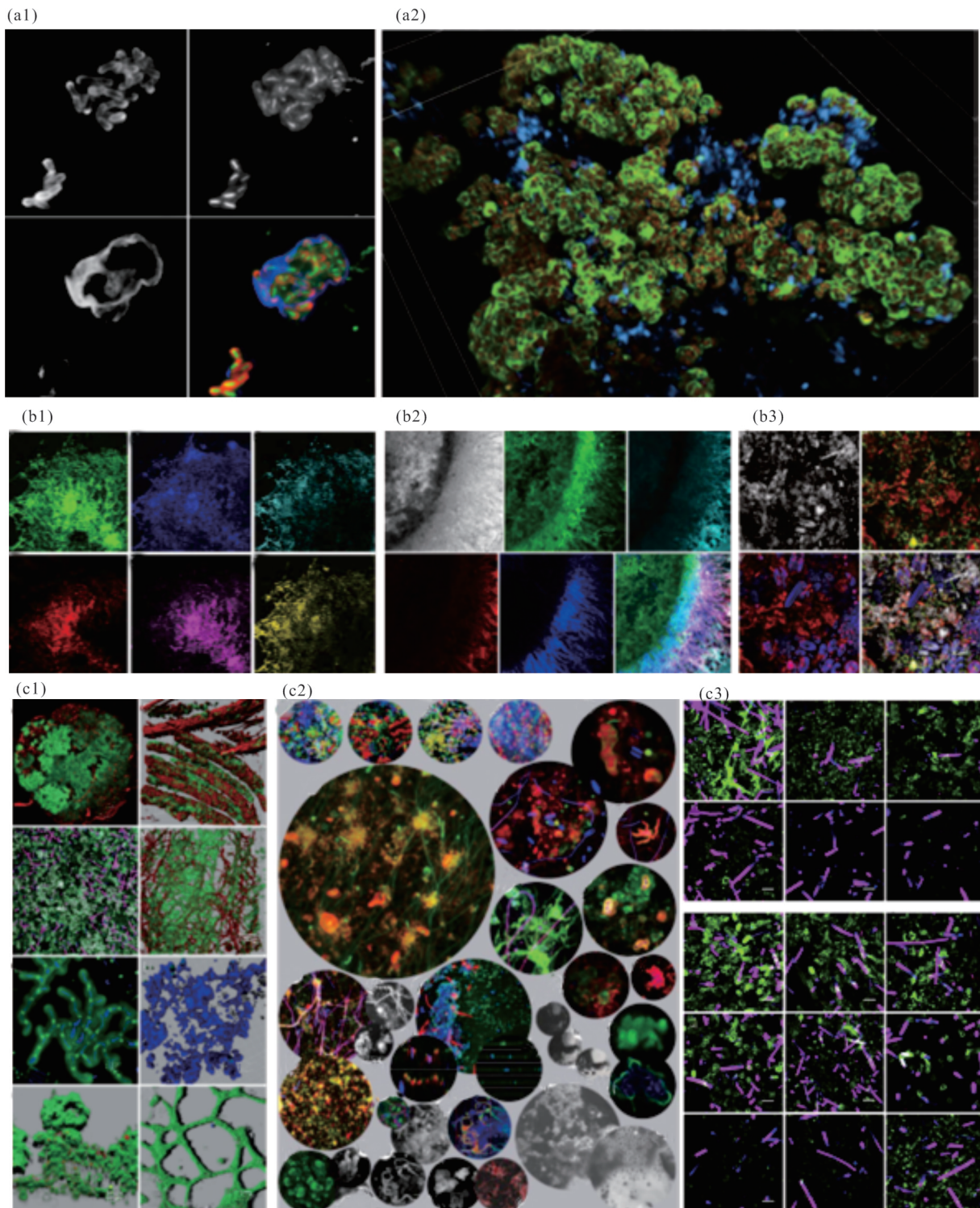
分析等, 最近 20 年逐步实现了地球与环境微生物原位微观组织结构 (Schramm et al., 2000; Haagensen et al., 2015)、胞内微环境 (Yeung et al., 2005)、胞外微环境 (Zhang and Bishop, 2001; Flemming et al., 2016)、矿物空间分布与微生物的相互关系 (Dong et al., 2009; Dong, 2010)、有机质和矿物相互关系 (图 7) (Gilbert et al., 2005)、矿物-有机质-微生物相互作用 (Huang, 2004; Huang et al., 2005, 2008)、微生物膜微环境 (Neu and Lawrence, 2014c)、微观 pH (图 8) (Hunter and Beveridge, 2005; Hidalgo et al., 2009; Hegler et al., 2010; Gashti et al., 2016) 以及  $p_{CO_2}$  (Schutting et al., 2014) 的原位分析等。激光扫描共聚焦显微镜应用于原位分析生物膜的结构组成和变化等 (Tolker-Nielsen and Molin, 2000) 特别是在分析 EPS 糖基、蛋白质、酶、胞外核酸、胞外微环境等方面 (Neu and Lawrence, 2014a, 2014b), 建立了凝集素结合原位分析糖缀合物的一系列方法标准 (Zippel and Neu, 2011; Neu and Lawrence, 2014c; Lawrence et al., 2016a) 对揭示生物膜群落微观尺度结构和功能 (Lawrence et al., 2004, 2012), 各种微生物群落



(a1) 微生物细胞-镉分布 (Johnson et al., 2018); (a2) 生物膜细胞-镍分布 (Wuertz et al., 2000); (a3) 微生物细胞-镉分布 (Ueshima et al., 2008); (a4) 生物膜锌的分布 (Hu et al., 2005); (b) 铁氧化过程中微生物细胞与金属离子、矿物质和胞外多糖的空间关系 (Que et al., 2008; Quang and Kim, 2010); (c1) 海洋微生物铁氧化过程中细胞与铁离子、矿物质和胞外多糖的关系 (Swanner et al., 2017); (c2) 海洋红球菌细胞-Fe(III)-矿物分布 (Wu et al., 2014)

图 6 激光扫描共聚焦显微镜分析微生物膜金属微观不均一性分布



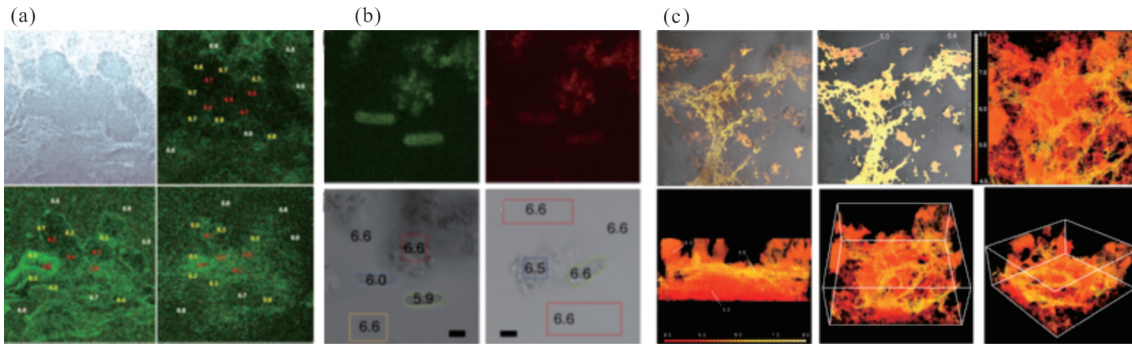


( a1) 不同多糖-细胞空间分布( Lawrence et al. ,2019) ; ( a2) 生物膜细胞外聚合物的空间分布( Flemming et al. ,2016) ; ( b1) 微生物颗粒蛋白质-β 多糖-α 多糖-总细胞-死细胞-脂质空间分布( Chen et al. ,2007a) ; ( b2) 微生物颗粒蛋白-α 多糖-核酸-β-多糖空间分布( Chen et al. ,2007b) ; ( b3) 河流生物膜反射-核酸-多糖-叶绿素 A 空间分布( Neu and Lawrence ,2014a ,2014b) ; ( c1) 不同生境的生物膜荧光凝集素结合分析( Neu and Lawrence ,2014a ,2014b) ; ( c2) 微生物生物膜结构、功能、微环境和分子组成; ( c3) 建立了凝集素结合原位分析糖缀合物的分析方法和标准( Zippel and Neu ,2011; Lawrence et al. ,2016a)

图 7 激光扫描共聚焦显微镜分析微生物膜微观结构和生化组成

Fig.7 Microstructures and biochemical compositions of microbial biofilms revealed by laser scanning





(a) 利用 C-SNARF-4 揭示生物膜-流体界面(黄色)和生物膜深处(红色)的 pH, 整个生物膜内的 pH 值微环境不连续(Hunter and Beveridge, 2005); (b) 利用 SNARF-4 揭示染色铁氧化细菌细胞外 pH 微环境原位分析。细胞的 pH=6.6, 背景 pH=6.6, 矿物质的 pH=6.5 (Hegler et al., 2010); (c) 二氧化硅纳米颗粒传感器的微生物生物膜中的 pH 微环境分析, 显示生物膜内存在相当大的异质性(Hidalgo et al., 2009)

图 8 激光扫描共聚焦显微镜分析微生物膜微环境 pH

Fig.8 pH values of micro-environments in microbial biofilm revealed by laser scanning confocal microscope analysis

EPS 分布、结构(Lawrence et al., 2005) 和作用(Yang et al., 2011a), 生物膜的时空化学组成变化(Milferstedt et al., 2007) 和物理结构(Milferstedt et al., 2009) 及其定量分析(Larimer et al., 2016) 等(图 7) 都起到了积极作用。

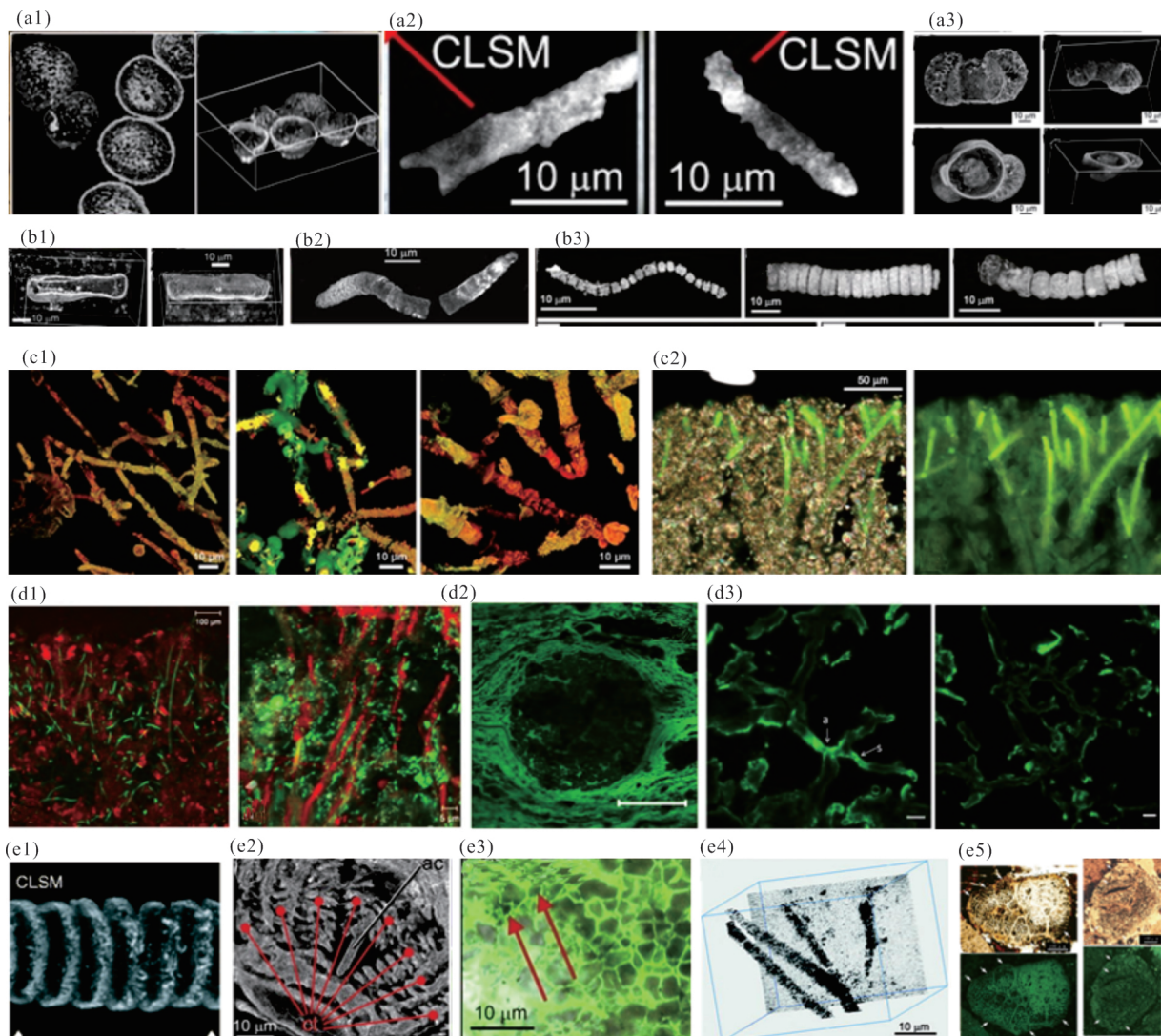
#### 4.3 微生物化石结构和组成

激光扫描共聚焦荧光显微镜技术很早就应用于地球科学领域(Scott, 1989), 目前集中在微生物化石表征上(Lepot, 2011; Foster et al., 2019)。该技术可以提供原位和亚微米级分辨率表征矿化微生物细胞形态, 提供非侵入性和非破坏性三维高分辨率和高保真度形态学信息(Schopf et al., 2006; Wacey, 2009) 和光谱学特征(Lepot, 2011), 揭示化石微观结构和形态(Belcher et al., 2013)、荧光物质分布(Chi et al., 2006; Kus, 2015) 和化学组成(Pan et al., 2019)。在寻找古代沉积岩中有机质的生物成因和同质性证据(Oehler and Cady, 2014) 方面, 通过激光扫描共聚焦荧光显微镜分析, 证明了新元古代页岩中真菌微化石细丝和菌丝体状结构残留壳有多糖的存在(Bonneville et al., 2020), 揭示了塔斯曼石切片有机物自发荧光光谱性质(Hackley et al., 2020) 和其热成熟度(Hackley and Kus, 2015), 揭示了现代微辉石中碳酸盐与微生物分子自发荧光的三维立体结构(Gérard et al., 2013)。近年来, 最引人注目的是古代显微化石激光扫描共聚焦荧光显微镜分析揭示出地球上最早化石的生物成因(Schopf and Kudryavtsev, 2009, 2012), 反映化石微生物群的微观组成(Schopf et al., 2010a), 如微生物细胞壁化石结构证据(Tewari, 2011)(图 9)。此外, 激光扫描共聚焦荧光显微镜也能对环境多孔介质进行三维成像(Shah et al., 2017), 揭

示胞外多糖土壤矿物质的相互作用(Lin et al., 2016), 还可用于气凝胶中彗星物质(Greenberg and Ebel, 2010)、油页岩(Nix and Feist-Burkhardt, 2003) 和琥珀的微观结构(Clark and Daly, 2010) 以及平面 pH 梯度分布(Rudd et al., 2005) 等研究。

## 5 展望

尽管激光扫描共聚焦显微镜技术联合荧光标记技术在地球生物学研究, 特别是重金属微观过程和机制、环境微生物膜微结构组成和微环境、微生物化石结构和组成方面做出了重要贡献。但由于其成像仅适用于半透明基质小样本(如环境微生物膜、岩石或琥珀切片的化石), 对不透明样品无效, 这很可能会限制其在地球微生物学中的应用。目前是采用两种或多种显微镜技术联用来弥补这一不足, 提供较传统单一技术更高精度的精细结构和组成信息。联用包括了方法技术联用和设备集成两个方面。前者如基于化学标记的光学显微镜和电子显微镜(Perkovic et al., 2014)、荧光显微镜和同步加速器 X 射线显微镜(Roudeau et al., 2014)、扫描电子显微镜和激光扫描共聚焦显微镜(Al-Nawas et al., 2001)、扫描透射 X 射线与激光扫描荧光显微镜(Naber et al., 2006)、拉曼光谱和激光扫描共聚焦显微镜(Pasteris et al., 2001) 联用能够揭示以往单一显微镜分析技术无法获得的微观信息。后者如荧光和扫描电子显微镜集成整合(Kanemaru et al., 2009) 和荧光和透射电子显微镜集成整合等(Agronskaia et al., 2008)。总之, 多种显微镜联用显微成像和设备集成技术(Matruglio et al., 2014) 可以更全面地展现微生物



(a1) 硅质岩岩石薄片中微化石 (Schopf et al., 2010b); (a2) 圆柱形丝状形态结构 (Schopf et al., 2017); (a3) 二叠纪矿化裸子植物花粉颗粒 (Schopf et al., 2016); (b1) 蓝藻化石 (Schopf, 2012); (b2) 蓝细菌化石 3D 形态 (Schopf, 2011); (b3) 蓝藻形态 (Schopf and Garcia, 2019); (c1) 白垩纪琥珀丝状微化石 (Martin and Martin, 2018); (c2) 凝灰岩叠层石包裹的丝状蓝细菌 (Shiraishi et al., 2008); (d1) 凝灰岩叠层生物膜 (Shiraishi et al., 2008); (d2) 油页岩微生物细胞 (Xie et al., 2015); (d3) 页岩中真菌微化石丝状结构 (Bonneville et al., 2020); (e1) 微化石三维结构 (Lepot, 2011); (e2) 八股胞特征的胚胎化石 (Schopf and Kudryavtsev, 2009); (e3) 岩石薄层中的原发藻 (Schopf and Kudryavtsev, 2012); (e4) 化石菌丝体三维结构 (Tewari, 2011); (e5) 藻类化石荧光三维结构 (Chi et al., 2006)

图9 激光扫描共聚焦显微镜分析古生物微化石结构和光谱特性

Fig.9 Structural and spectral characteristics of paleontological microfossils revealed by laser scanning confocal microscope analysis

膜的物理结构和化学组成 (Obst and Schmid, 2014; Schmid et al., 2014)、有机和无机微环境相互作用 (Hunter, 2009) 克服单一显微镜分析技术无法获得的微观信息, 这必将极大地促进地球生物学的发展。

致谢: 中国科学院地球化学研究所领导和同事对初稿提出了建设性意见和建议, 课题组博士研究生付玉聪、杨慧、刘灵飞, 硕士研究生江娜、邵凯瑞、卢嘉珩、黄强、李宝同学对手稿准备提供了帮助, 在此一并致谢。

参考文献 (References):

Ackerman C M, Lee S, Chang C J. 2017. Analytical methods for imaging metals in biology: From transition metal metabolism to transition metal signaling. *Analytical Chemistry*, 89(1): 22-41

Adams M C, Salmon W C, Gupton S L, Cohan C S, Wittmann T, Prig-ozhina N, Waterman-Storer C M. 2003. A high-speed multispectral spinning-disk confocal microscope system for fluorescent speckle microscopy of living cells. *Methods*, 29(1): 29-41

Agronskaia A V, Valentijn J A, Van Driel L F, Schneijdenberg C T W M, Humbel B M, Van Bergen en Henegouwen P M P, Verkleij A J, Koster A J, Gerritsen H C. 2008. Integrated fluorescence and

- transmission electron microscopy. *Journal of Structural Biology*, 164 (2): 183–189
- Alberts B, Johnson A, Lewis J, Raff M, Roberts K, Walter P. 2002. *Molecular biology of the cell*. 4th ed. New York: Garland Science
- Al-Nawas B, Grötz K A, Götz H, Heinrich G, Rippin G, Stender E, Duschner H, Wagner W. 2001. Validation of three-dimensional surface characterising methods: Scanning electron microscopy and confocal laser scanning microscopy. *Scanning*, 23(4): 227–231
- Anderson R R, Webb R H, Rajadhyaksha M. 1999. Three-dimensional scanning confocal laser microscope: US, 19068998: A
- Baker M. 2011. Microscopy: Bright light, better labels. *Nature*, 478 (7367): 137–142
- Baleizao C, Nagl S, Schäferling M, Berberan-Santos M N, Wolfbeis O S. 2008. Dual fluorescence sensor for trace oxygen and temperature with unmatched range and sensitivity. *Analytical Chemistry*, 80(16): 6449–6457
- Bao X F, Cao Q S, Nie X M, Zhou Y M, Ye R L, Zhou B J, Zhu J. 2015a. Design and synthesis of a novel chromium(III). Selective fluorescent chemosensor bearing a thiodiacetamide moiety and two rhodamine B fluorophores. *Sensors and Actuators B: Chemical*, 221: 930–939
- Bao X F, Cao Q S, Xu Y Z, Gao Y X, Xu Y, Nie X M, Zhou B J, Pang T, Zhu J. 2015b. Synthesis and evaluation of a new Rhodamine B and Di(2-picolyl) amine conjugate as a highly sensitive and selective chemosensor for Al<sup>3+</sup> and its application in living-cell imaging. *Bioorganic & Medicinal Chemistry*, 23(4): 694–702
- Beija M, Afonso C A M, Martinho J M G. 2009. Synthesis and applications of Rhodamine derivatives as fluorescent probes. *Chemical Society Reviews*, 38(8): 2410–2433
- Belcher C M, Punyasena S W, Sivaguru M. 2013. Novel application of confocal laser scanning microscopy and 3D volume rendering toward improving the resolution of the fossil record of charcoal. *PLoS One*, 8(8): e72265
- Bester E, Kroukamp O, Wolfaardt G M, Boonzaaier L, Liss S N. 2010. Metabolic differentiation in biofilms as indicated by carbon dioxide production rates. *Applied and Environmental Microbiology*, 76(4): 1189–1197
- Biswal B, Mallick D, Thirunavoukkarasu M, Mohanty R, Bag B. 2016. A pyridine and pyrrole coupled rhodamine derivative for Co(II) ion detection and its imaging application in plant tissues. *Sensors and Actuators B: Chemical*, 232: 410–419
- Boens N, Leen V, Dehaen W, Wang L N, Robeyns K, Qin W W, Tang X L, Beljonne D, Tonnele C, Paredes J M, Ruedas-Rama M J, Orte A, Crovetto L, Talavera E M, Alvarez-Pez J M. 2012. Visible Absorption and Fluorescence Spectroscopy of Conformationally Constrained, Annulated BODIPY Dyes. *Journal of Physical Chemistry A*, 116(39): 9621–9631
- Bonneville S, Delpomdor F, Préat A, Chevalier C, Araki T, Kazemian M, Steele A, Schreiber A, Wirth R, Benning L G. 2020. Molecular identification of fungi microfossils in a Neoproterozoic shale rock. *Science Advances*, 6(4): eaax7599
- Boudoux C, Yun S H, Oh W Y, White W M, Hftimia N V, Shishkov M, Bouma B E, Tearney G J. 2005. Rapid wavelength-swept spectrally encoded confocal microscopy. *Optics Express*, 13(20): 8214–8221
- Bridier A, Briandet R. 2014. Contribution of confocal laser scanning microscopy in deciphering biofilm tridimensional structure and reactivity. In: Donelli G, ed. *Microbial Biofilms: Methods and Protocols*. New York: Springer, 255–266
- Brismar H, Ulfhake B. 1997. Fluorescence lifetime measurements in confocal microscopy of neurons labeled with multiple fluorophores. *Nature Biotechnology*, 15(4): 373–377
- Brockmann S, Arnold T, Schweder B, Bernhard G. 2010. Visualizing acidophilic microorganisms in biofilm communities using acid stable fluorescence dyes. *Journal of Fluorescence*, 20(4): 943–951
- Brown C M. 2007. Fluorescence microscopy—avoiding the pitfalls. *Journal of Cell Science*, 120(10): 1703–1705
- Caldwell D E, Korber D R, Lawrence J R. 1992. Confocal laser microscopy and digital image analysis in microbial ecology. In: Marshall K C, ed. *Advances in Microbial Ecology*. Boston: Springer, 1–67
- Caplan J, Niethammer M, Taylor II R M, Czymbek K J. 2011. The power of correlative microscopy: Multi-modal, multi-scale, multi-dimensional. *Current Opinion in Structural Biology*, 21(5): 686–693
- Carlsson K, Danielsson P E, Lenz R, Liljeborg A, Majlöf L, Åslund N. 1985. Three-dimensional microscopy using a confocal laser scanning microscope. *Optics Letters*, 10(2): 53–55
- Carlsson K, Åslund N, Mossberg K, Philip J. 1994. Simultaneous confocal recording of multiple fluorescent labels with improved channel separation. *Journal of Microscopy*, 176(3): 287–299
- Carter K P, Young A M, Palmer A E. 2014. Fluorescent sensors for measuring metal ions in living systems. *Chemical Reviews*, 114(8): 4564–4601
- Castellano-Muñoz M, Peng A W, Salles F T, Ricci A J. 2012. Swept field laser confocal microscopy for enhanced spatial and temporal resolution in live-cell imaging. *Microscopy and Microanalysis*, 18(4): 753–760
- Cavaliere C, Aiello M, Torino E, Mollo V, Marcello L, De Luca D, Di Spinazzola N P, Parlato V, Netti P A. 2016. Advanced imaging techniques. In: Sacerdoti F M, Giordano A, Cavaliere C, eds. *Advanced Imaging Techniques in Clinical Pathology*. New York: Humana Press, 85–104
- Chang H T, Rittmann B E. 1986. Biofilm loss during sample preparation for scanning electron microscopy. *Water Research*, 20(11): 1451–1456
- Chansawang N, Obara B, Geider R J, Laissue P P. 2016. Three-dimensional visualisation and quantification of lipids in microalgae using confocal laser scanning microscopy. In: McGenity T J, Timmis K N, Nogales B, eds. *Hydrocarbon and Lipid Microbiology Protocols: Ultrastructure and Imaging*. Berlin: Springer, 145–161
- Chatterjee A, Santra M, Won N, Kim S, Kim J K, Kim S B, Ahn K H. 2009. Selective fluorogenic and chromogenic probe for detection of silver ions and silver nanoparticles in aqueous media. *Journal of the American Chemical Society*, 131(6): 2040–2041
- Chen M Y, Lee D J, Yang Z, Peng X F, Lai J Y. 2006. Fluorescent staining for study of extracellular polymeric substances in membrane biofouling layers. *Environmental Science & Technology*, 40(21): 6642–6646
- Chen M Y, Lee D J, Tay J H, Show K Y. 2007a. Staining of

- extracellular polymeric substances and cells in bioaggregates. *Applied Microbiology and Biotechnology*, 75(2): 467–474
- Chen M Y, Lee D J, Tay J H. 2007b. Distribution of extracellular polymeric substances in aerobic granules. *Applied Microbiology and Biotechnology*, 73(6): 1463–1469
- Chen X L, Meng X M, Wang S X, Cai Y L, Wu Y F, Feng Y, Zhu M Z, Guo Q X. 2013. A rhodamine-based fluorescent probe for detecting  $\text{Hg}^{2+}$  in a fully aqueous environment. *Dalton Transactions*, 42(41): 14819–14825
- Chen X Q, Tian X Z, Shin I, Yoon J. 2011. Fluorescent and luminescent probes for detection of reactive oxygen and nitrogen species. *Chemical Society Reviews*, 40(9): 4783–4804
- Chen Y, Chen B, Han Y F. 2016. A novel rhodamine-based fluorescent probe for the fluorogenic and chromogenic detection of  $\text{Pd}^{2+}$  ions and its application in live-cell imaging. *Sensors and Actuators B: Chemical*, 237: 1–7
- Cheng J Y, Yang E B, Ding P G, Tang J, Zhang D, Zhao Y F, Ye Y. 2015. Two rhodamine based chemosensors for  $\text{Sn}^{4+}$  and the application in living cells. *Sensors and Actuators B: Chemical*, 221: 688–693
- Chi H M, Xiao Z D, Fu D G, Lu Z H. 2006. Analysis of fluorescence from algae fossils of the Neoproterozoic Doushantuo formation of China by confocal laser scanning microscope. *Microscopy Research and Technique*, 69(4): 253–259
- Clark N D L, Daly C J. 2010. Using confocal laser scanning microscopy to image trichome inclusions in amber. *Journal of Paleontological Techniques*, 8: 1–7
- Clifford J N, Bell T D M, Tinnefeld P, Heilemann M, Melnikov S M, Hotta J I, Sliwa M, Dedecker P, Sauer M, Hofkens J, Yeow E K L. 2007. Fluorescence of single molecules in polymer films: Sensitivity of blinking to local environment. *The Journal of Physical Chemistry B*, 111(25): 6987–6991
- Cowan S E, Gilbert E, Khlebnikov A, Keasling J D. 2000. Dual labeling with green fluorescent proteins for confocal microscopy. *Applied and Environmental Microbiology*, 66(1): 413–418
- Croft W J. 2006. Under the microscope: A brief history of microscopy. Hackensack: World Scientific
- Cullander C. 1999. Fluorescent probes for confocal microscopy. In: Pad-dock S W, ed. *Confocal Microscopy Methods and Protocols*. Totowa: Humana Press, 59–73
- Czarnik A W. 1998. A sense for landmines. *Nature*, 394(6692): 417–418
- Daly C J, Parmryd I, McGrath J C. 2012. Visualization and analysis of vascular receptors using confocal laser scanning microscopy and fluorescent ligands. In: Davenport A P, ed. *Receptor Binding Techniques*. Totowa: Humana Press, 95–107
- De A K, Goswami D. 2009. Adding new dimensions to laser-scanning fluorescence microscopy. *Journal of Microscopy*, 233(2): 320–325
- Delpiano J, Jara J, Scheer J, Ramírez O A, Ruiz-del-Solar J, Härtel S. 2012. Performance of optical flow techniques for motion analysis of fluorescent point signals in confocal microscopy. *Machine Vision and Applications*, 23(4): 675–689
- Dey N, Blanc-Feraud L, Zimmer C, Roux P, Kam Z, Olivo-Marín J C, Zerubia J. 2006. Richardson-Lucy algorithm with total variation regularization for 3D confocal microscope deconvolution. *Microscopy Research and Technique*, 69(4): 260–266
- Dohnalkova A C, Marshall M J, Arey B W, Williams K H, Buck E C, Fredrickson J K. 2011. Imaging hydrated microbial extracellular polymers: Comparative analysis by electron microscopy. *Applied and Environmental Microbiology*, 77(4): 1254–1262
- Domaille D W, Que E L, Chang C J. 2008. Synthetic fluorescent sensors for studying the cell biology of metals. *Nature Chemical Biology*, 4(3): 168–175
- Dong H L, Jaisi D P, Kim J, Zhang G X. 2009. Microbe-clay mineral interactions. *American Mineralogist*, 94(11–12): 1505–1519
- Dong H L. 2010. Mineral-microbe interactions: A review. *Frontiers of Earth Science in China*, 4(2): 127–147
- Dong L, Wu C, Zeng X, Mu L, Xue S F, Tao Z, Zhang J X. 2010. The synthesis of a rhodamine B Schiff-base chemosensor and recognition properties for  $\text{Fe}^{3+}$  in neutral ethanol aqueous solution. *Sensors and Actuators B: Chemical*, 145(1): 433–437
- Downie H F, Valentine T A, Otten W, Spiers A J, Dupuy L X. 2014. Transparent soil microcosms allow 3D spatial quantification of soil microbiological processes *in vivo*. *Plant Signaling & Behavior*, 9(10): e970421
- Drepper T, Eggert T, Circolone F, Heck A, Krauß U, Guterl J K, Wendorf M, Losi A, Gärtner W, Jaeger K E. 2007. Reporter proteins for *in vivo* fluorescence without oxygen. *Nature Biotechnology*, 25(4): 443–445
- Du P W, Lippard S J. 2010. A highly selective turn-on colorimetric, red fluorescent sensor for detecting mobile zinc in living cells. *Inorganic Chemistry*, 49(23): 10753–10755
- Dutta S, Flottmann B, Heilemann M, Mokhir A. 2012. Hybridization and reaction-based fluorogenic nucleic acid probes. *Chemical Communications*, 48(77): 9664–9666
- Emrullahoğlu M, Karakus E, Üçüncü M. 2013. A rhodamine based "turn-on" chemodosimeter for monitoring gold ions in synthetic samples and living cells. *Analyst*, 138(13): 3638–3641
- Ezeh V C, Harrop T C. 2012. A sensitive and selective fluorescence sensor for the detection of arsenic(III) in organic media. *Inorganic Chemistry*, 51(3): 1213–1215
- Fahrni C J. 2013. Synthetic fluorescent probes for monovalent copper. *Current Opinion in Chemical Biology*, 17(14): 656–662
- Fernández-Suárez M, Ting A Y. 2008. Fluorescent probes for super-resolution imaging in living cells. *Nature Reviews Molecular Cell Biology*, 9(12): 929–943
- Ferrari L, Rovati L, Fabbri P, Pilati F. 2013. Disposable fluorescence optical pH sensor for near neutral solutions. *Sensors*, 13(1): 484–499
- Fili N, Toseland C P. 2014. Fluorescence and labelling: How to choose and what to do. In: Toseland C P, Fili N, eds. *Fluorescent Methods for Molecular Motors*. Basel: Springer, 1–24
- Flemming H C, Neu T R, Wingender J. 2016. The perfect slime: Microbial extracellular polymeric substances (EPS). London: IWA Publishing
- Földes-Papp Z, Demel U, Tilz G P. 2003. Laser scanning confocal fluorescence microscopy: An overview. *International Immunopharmacology*, 3(13–14): 1715–1729



- Foster J S , Reid R P , Visscher P T , Dupraz C. 2019. Characterizing modern microbialites and the geobiological processes underlying their formation. *Frontiers in Microbiology* , 10: 2299
- Fricker M , Runions J , Moore I. 2006. Quantitative fluorescence microscopy: From Art to Science. *Annual Review of Plant Biology* , 57: 79–107
- Garini Y , Young I T , McNamara G. 2006. Spectral imaging: Principles and applications. *Cytometry Part A* , 69A( 8) : 735–747
- Gashti M P , Asselin J , Barbeau J , Boudreau D , Greener J. 2016. A microfluidic platform with pH imaging for chemical and hydrodynamic stimulation of intact oral biofilms. *Lab on a Chip* , 16( 18) : 1412–1419
- Ge F Y , Chen L G. 2008. pH fluorescent probes: Chlorinated fluoresceins. *Journal of Fluorescence* , 18( 3–4) : 741–747
- Gérard E , Ménez B , Couradeau E , Moreira D , Benzerara K , Tavera R , López-García P. 2013. Specific carbonate-microbe interactions in the modern microbialites of Lake Alchichica ( Mexico) . *The ISME Journal* , 7( 10) : 1997–2009
- Greenberg M , Ebel D S. 2010. Laser scanning confocal microscopy of Stardust material. *Geosphere* , 6( 5) : 515–523
- Gilbert P U P A , Abrecht M , Frazer B H. 2005. The organic-mineral interface in biominerals. *Reviews in Mineralogy and Geochemistry* , 59( 1) : 157–185
- Gitai Z. 2009. New fluorescence microscopy methods for microbiology: Sharper , faster , and quantitative. *Current Opinion in Microbiology* , 12( 3) : 341–346
- Gomes A , Fernandes E , Lima J L F C. 2005. Fluorescence probes used for detection of reactive oxygen species. *Journal of Biochemical and Biophysical Methods* , 65( 2–3) : 45–80
- Gomes A , Fernandes E , Lima J L F C. 2006. Use of fluorescence probes for detection of reactive nitrogen species: A review. *Journal of Fluorescence* , 16: 119–139
- Gonçalves M S T. 2009. Fluorescent labeling of biomolecules with organic probes. *Chemical Reviews* , 109( 1) : 190–212
- Gould T J , Gunewardene M S , Gudheti M V , Verkhusha V V , Yin S R , Gosse J A , Hess S T. 2008. Nanoscale imaging of molecular positions and anisotropies. *Nature Methods* , 5( 12) : 1027–1030
- Grimm J B , Heckman L M , Lavis L D. 2013. Chapter one-the chemistry of small-molecule fluorogenic probes. *Progress in Molecular Biology and Translational Science*. 113: 1–34
- Guo Z Q , Park S , Yoon J , Shin I. 2014. Recent progress in the development of near-infrared fluorescent probes for bioimaging applications. *Chemical Society Reviews* , 43( 1) : 16–29
- Gupta V K , Mergu N , Kumawat L K , Singh A K. 2015. A reversible fluorescence “off-on-off” sensor for sequential detection of aluminum and acetate/fluoride ions. *Talanta* , 144: 80–89
- Haagensen J A J , Hansen S K , Christensen B B , Pamp S J , Molin S. 2015. Development of spatial distribution patterns by biofilm cells. *Applied and Environmental Microbiology* , 81( 18) : 6120–6128
- Haaland D M , Jones H D T , Van Benthem M H , Sinclair M B , Melgaard D K , Stork C L , Pedroso M C , Liu P , Brasier A R , Andrews N L , Lidke D S. 2009. Hyperspectral confocal fluorescence imaging: Exploring alternative multivariate curve resolution approaches. *Applied Spectroscopy* , 63( 3) : 271–279
- Hackley P C , Kus J. 2015. Thermal maturity of *Tasmanites* microfossils from confocal laser scanning fluorescence microscopy. *Fuel* , 143: 343–350
- Hackley P C , Jubb A M , Burruss R C , Beaven A E. 2020. Fluorescence spectroscopy of ancient sedimentary organic matter via confocal laser scanning microscopy ( CLSM) . *International Journal of Coal Geology* , 223: 103445
- Halan B , Buehler K , Schmid A. 2012. Biofilms as living catalysts in continuous chemical syntheses. *Trends in Biotechnology* , 30( 9) : 453–465
- Han J Y , Burgess K. 2010. Fluorescent indicators for intracellular pH. *Chemical Reviews* , 110( 5) : 2709–2728
- Hao L K , Li J L , Kappler A , Obst M. 2013. Mapping of heavy metal ion sorption to cell-extracellular polymeric substance-mineral aggregates by using metal-selective fluorescent probes and confocal laser scanning microscopy. *Applied and Environmental Microbiology* , 79( 21) : 6524–6534
- Hao L K , Guo Y , Byrne J M , Zeitvogel F , Schmid G , Ingino P , Li J L , Neu T R , Swanner E D , Kappler A , Obst M. 2016. Binding of heavy metal ions in aggregates of microbial cells , EPS and biogenic iron minerals measured *in-situ* using metal- and glycoconjugates-specific fluorophores. *Geochimica et Cosmochimica Acta* , 180: 66–96
- Haraguchi T , Shimi T , Koujin T , Hashiguchi N , Hiraoka Y. 2002. Spectral imaging fluorescence microscopy. *Genes to Cells* , 7( 9) : 881–887
- Hawkes P W , Spence J C H. 2007. *Science of microscopy*. New York: Springer
- Hegler F , Schmidt C , Schwarz H , Kappler A. 2010. Does a low-pH microenvironment around phototrophic Fe<sup>II</sup>-oxidizing bacteria prevent cell encrustation by Fe<sup>III</sup> minerals? *FEMS Microbiology Ecology* , 74( 3) : 592–600
- Herbert S , Bouchet B , Riaublanc A , Dufour E , Gallant D J. 1999. Multiple fluorescence labelling of proteins , lipids and whey in dairy products using confocal microscopy. *Le Lait* , 79( 6) : 567–575
- Hidalgo G , Burns A , Herz E , Hay A G , Houston P L , Wiesner U , Lion L W. 2009. Functional tomographic fluorescence imaging of pH microenvironments in microbial biofilms by use of silica nanoparticle sensors. *Applied and Environmental Microbiology* , 75( 23) : 7426–7435
- Hille C , Berg M , Bressel L , Munzke D , Primus P , Löhmannsröben H G , Dosche C. 2008. Time-domain fluorescence lifetime imaging for intracellular pH sensing in living tissues. *Analytical and Bioanalytical Chemistry* , 391( 5) : 1871–1879
- Hiraoka Y , Shimi T , Haraguchi T. 2002. Multispectral imaging fluorescence microscopy for living cells. *Cell Structure and Function* , 27( 5) : 367–374
- Hirayama T , Okuda K , Nagasawa H. 2013. A highly selective turn-on fluorescent probe for iron( II) to visualize labile iron in living cells. *Chemical Science* , 4( 3) : 1250–1256
- Hoffman R M. 2005. The multiple uses of fluorescent proteins to visualize cancer *in vivo*. *Nature Reviews Cancer* , 5( 10) : 796–806
- Hori Y , Kikuchi K. 2013. Protein labeling with fluorogenic probes for no-wash live-cell imaging of proteins. *Current Opinion in Chemical Biol-*



- ogy, 17(4): 644–650
- Hou G G, Wang C H, Sun J F, Yang M Z, Lin D, Li H J. 2013. Rhodamine-based “turn-on” fluorescent probe with high selectivity for  $\text{Fe}^{2+}$  imaging in living cells. *Biochemical and Biophysical Research Communications*, 439(4): 459–463
- Hu Z Q, Hidalgo G, Houston P L, Hay A G, Shuler M L, Abruña H D, Ghiorse W C, Lion L W. 2005. Determination of spatial distributions of zinc and active biomass in microbial biofilms by two-photon laser scanning microscopy. *Applied and Environmental Microbiology*, 71(7): 4014–4021
- Hu Z Q, Jin J, Abruña H D, Houston P L, Hay A G, Ghiorse W C, Shuler M L, Hidalgo G, Lion L W. 2007. Spatial distributions of copper in microbial biofilms by scanning electrochemical microscopy. *Environmental Science & Technology*, 41(3): 936–941
- Huang L, Hou F P, Xi P X, Bai D C, Xu M, Li Z P, Xie G Q, Shi Y J, Liu H Y, Zeng Z Z. 2011. A rhodamine-based “turn-on” fluorescent chemodosimeter for  $\text{Cu}^{2+}$  and its application in living cell imaging. *Journal of Inorganic Biochemistry*, 105(6): 800–805
- Huang P M. 2004. Soil mineral-organic matter-microorganism interactions: fundamentals and impacts. *Advances in Agronomy*, 82: 391–472
- Huang P M, Wang M K, Chiu C Y. 2005. Soil mineral-organic matter-microbe interactions: Impacts on biogeochemical processes and biodiversity in soils. *Pedobiologia*, 49(6): 609–635
- Huang Q Y, Huang P M, Violante A. 2008. Soil mineral microbe-organic interactions: Theories and applications. Berlin: Springer
- Hughes L D, Rawle R J, Boxer S G. 2014. Choose your label wisely: Water-soluble fluorophores often interact with lipid bilayers. *PLoS One*, 9: e87649
- Hunter R. 2009. Biofilms, minerals, and bronchioles: Understanding microenvironments through correlative microscopy. *Microscopy and Microanalysis*, 15(S2): 68–69
- Hunter R C, Beveridge T J. 2005. Application of a pH-sensitive fluorophore (C-SNARF-4) for pH microenvironment analysis in *Pseudomonas aeruginosa* biofilms. *Applied and Environmental Microbiology*, 71(5): 2501–2510
- Hunter R C, Beveridge T J. 2008. Metal-bacteria interactions at both the planktonic cell and biofilm levels. In: Sigel A, Sigel H, Sigel R K O, eds. *Bio-mineralization: From Nature to Application*. Chichester: John Wiley & Sons, 127–165
- Huo F J, Su J, Sun Y Q, Yin C X, Tong H B, Nie Z X. 2010. A rhodamine-based dual chemosensor for the visual detection of copper and the ratiometric fluorescent detection of vanadium. *Dyes and Pigments*, 86(1): 50–55
- Icha J, Weber M, Waters J C, Norden C. 2017. Phototoxicity in live fluorescence microscopy, and how to avoid it. *BioEssays*, 39(8): 1700003
- Jaiswal J K, Mattoussi H, Mauro J M, Simon S M. 2003. Long-term multiple color imaging of live cells using quantum dot bioconjugates. *Nature Biotechnology*, 21: 47–51
- Jensen E C. 2012. Use of fluorescent probes: Their effect on cell biology and limitations. *The Anatomical Record*, 295(12): 2031–2036
- Johnson C R, Shrout J D, Fein J B. 2018. Visualization and quantification of Cd sorption to bacteria using confocal laser scanning microscopy and Cd-specific fluorescent probes. *Chemical Geology*, 483: 21–30
- Johnson I D. 2006. Practical considerations in the selection and application of fluorescent probes. In: Pawley J B, ed. *Handbook of Biological Confocal Microscopy*. Boston: Springer, 353–367
- Johnsson N, Johnsson K. 2007. Chemical tools for biomolecular imaging. *ACS Chemical Biology*, 2(1): 31–38
- Jou M J, Chen X Q, Swamy K M K, Kim H N, Kim H J, Lee S G, Yoon J. 2009. Highly selective fluorescent probe for  $\text{Au}^{3+}$  based on cyclization of propargylamide. *Chemical Communications*, (46): 7218–7220
- Julien C, Laurent E, Legube B, Thomassin J H, Mondamert L, Labanowski J. 2014. Investigation on the iron-uptake by natural biofilms. *Water Research*, 50: 212–220
- Kaestner L. 2013. Fluorescence-based visualization. In: Kaestner L, ed. *Calcium Signalling*. Berlin: Springer, 4–13
- Kamburoğlu K, Barenboim S F, Arntürk T, Kaffe I. 2008. Quantitative measurements obtained by micro-computed tomography and confocal laser scanning microscopy. *Dentomaxillofacial Radiology*, 37(7): 385–391
- Kanemaru T, Hirata K, Takasu S I, Isobe S I, Mizuki K, Mataka S, Nakamura K I. 2009. A fluorescence scanning electron microscope. *Ultramicroscopy*, 109(4): 344–349
- Kang N Y, Ha H H, Yun S W, Yu Y H, Chang Y T. 2011. Diversity-driven chemical probe development for biomolecules: Beyond hypothesis-driven approach. *Chemical Society Reviews*, 40(7): 3613–3626
- Karakuş E, Üçüncü M, Emrullahoğlu M. 2013. A rhodamine/Bodipy-based fluorescent probe for the differential detection of  $\text{Hg}(\text{II})$  and  $\text{Au}(\text{III})$ . *Chemical Communications*, 50(9): 1119–1121
- Kawaguchi T, Decho A W. 2002. In situ microspatial imaging using two-photon and confocal laser scanning microscopy of bacteria and extracellular polymeric secretions (EPS) within marine stromatolites. *Marine Biotechnology*, 4(2): 127–131
- Kermis H R, Kostov Y, Harms P, Rao G. 2002. Dual excitation ratio-metric fluorescent pH sensor for noninvasive bioprocess monitoring: Development and application. *Biotechnology Progress*, 18(5): 1047–1053
- Kikuchi K, Komatsu K, Nagano T. 2004. Zinc sensing for cellular application. *Current Opinion in Chemical Biology*, 8(2): 182–191
- Kikuchi K. 2010. Design, synthesis and biological application of chemical probes for bio-imaging. *Chemical Society Reviews*, 39(6): 2048–2053
- Kim H, Lee S, Lee J, Tae J. 2010. Rhodamine triazole-based fluorescent probe for the detection of  $\text{Pt}^{2+}$ . *Organic Letters*, 12(22): 5342–5345
- Kim H M, Cho B R. 2011. Two-photon fluorescent probes for metal ions. *Chemistry-an Asian Journal*, 6(1): 58–69
- Kim H N, Ren W X, Kim J S, Yoon J. 2012. Fluorescent and colorimetric sensors for detection of lead, cadmium, and mercury ions. *Chemical Society Reviews*, 41(8): 3210–3244
- Kumar M, Kumar N, Bhalla V. 2011. FRET-induced nanomolar detection of  $\text{Fe}^{2+}$  based on cinnamaldehyde-rhodamine derivative. *Tetrahedron Letters*, 52(33): 4333–4336

- Kumar N , Bhalla V , Kumar M. 2013. Recent developments of fluorescent probes for the detection of gasotransmitters( NO , CO and H<sub>2</sub>S) . *Coordination Chemistry Reviews* , 257( 15-16) : 2335-2347
- Kus J. 2015. Application of confocal laser-scanning microscopy( CLSM) to autofluorescent organic and mineral matter in peat , coals and siliciclastic sedimentary rocks: A qualitative approach. *International Journal of Coal Geology* , 137: 1-18
- Kwon J Y , Jang Y J , Lee Y J , Kim K M , Seo M S , Nam W , Yoon J. 2005. A highly selective fluorescent chemosensor for Pb<sup>2+</sup>. *Journal of the American Chemical Society* , 127( 28) : 10107-10111
- Lacivita E , Leopoldo M , Berardi F , Colabufo N A , Perrone R. 2012. Activatable fluorescent probes: A new concept in optical molecular imaging. *Current Medicinal Chemistry* , 19( 28) : 4731-4741
- Legendijk E L , Validov S , Lamers G E M , De Weert S , Bloemberg G V. 2010. Genetic tools for tagging Gram-negative bacteria with mCherry for visualization *in vitro* and in natural habitats , biofilm and pathogenicity studies. *FEMS Microbiology Letters* , 305( 1) : 81-90
- Lang K , Chin J W. 2013. Shining a light into live cells. *Nature Chemistry* , 5( 2) : 81-82
- Larimer C , Winder E , Jeters R , Prowant M , Nettleship I , Addleman R S , Bonheyo G T. 2016. A method for rapid quantitative assessment of biofilms with biomolecular staining and image analysis. *Analytical and Bioanalytical Chemistry* , 408( 3) : 999-1008
- Laurent M , Johannin G , Gilbert N , Lucas L , Cassio D , Petit P X , Fleury A. 1994. Power and limits of laser scanning confocal microscopy. *Biology of the Cell* , 80( 2-3) : 229-240
- Lavis L D , Chao T Y , Raines R T. 2006. Fluorogenic label for biomolecular imaging. *ACS Chemical Biology* , 1( 4) : 252-260
- Lavis L D , Raines R T. 2008. Bright ideas for chemical biology. *ACS Chemical Biology* , 3( 3) : 142-155
- Lawrence J R , Chenier M R , Roy R , Beaumier D , Fortin N , Swerhone G D W , Neu T R , Greer C W. 2004. Microscale and molecular assessment of impacts of nickel , nutrients , and oxygen level on structure and function of river biofilm communities. *Applied and Environmental Microbiology* , 70( 7) : 4326-4339
- Lawrence J R , Hitchcock A P , Leppard G G , Neu T R. 2001. Mapping biopolymer distributions in microbial communities [J]. *Ibm Systems Journal* , 40( 4) : 831-841
- Lawrence J R , Zhu B , Swerhone G D W , Roy J , Tumber V , Waiser M J , Topp E , Korber D R. 2012. Molecular and microscopic assessment of the effects of caffeine , acetaminophen , diclofenac , and their mixtures on river biofilm communities. *Environmental Toxicology and Chemistry* , 31( 3) : 508-517
- Lawrence J R , Neu T R , Paule A , Korber D R , Wolfaardt G. 2016a. Aquatic biofilms: Development , cultivation , analyses , and applications. In: Yates M , Nakatsu C , Miller R , Pillai S , eds. *Manual of Environmental Microbiology* , 4th ed. Washington: ASM Press
- Lawrence J R , Swerhone G D W , Kuhlicke U , Neu T R. 2016b. *In situ* evidence for metabolic and chemical microdomains in the structured polymer matrix of bacterial microcolonies. *FEMS Microbiology Ecology* , 92( 11) : fiw183
- Lawrence J R , Swerhone G D W , Neu T R. 2019. Visualization of the sorption of nickel within exopolymer microdomains of bacterial microcolonies using confocal and scanning electron microscopy. *Microbes and Environments* , 34( 1) : 76-82
- Lee J S , Vendrell M , Chang Y T. 2011. Diversity-oriented optical imaging probe development. *Current Opinion in Chemical Biology* , 15( 6) : 760-767
- Lepot K. 2011. Microfossils , analytical techniques. In: Gargaud M , Amils R , Quintanilla J C , Cleaves II H J , Irvine W M , Pinti D L , Viso M , eds. *Encyclopedia of Astrobiology*. Berlin: Springer , 1049-1054
- Li CY , Felz S , Wagner M , Lackner S , Horn H. 2016. Investigating biofilm structure developing on carriers from lab-scale moving bed biofilm reactors based on light microscopy and optical coherence tomography. *Bioresource Technology* , 200: 128-136
- Li H L , Fan J L , Du J J , Guo K X , Sun S G , Liu X J , Peng X J. 2010. A fluorescent and colorimetric probe specific for palladium detection. *Chemical Communications* , 46( 7) : 1079-1081
- Li M , Zhang D , Liu Y Q , Ding P G , Ye Y , Zhao Y F. 2014a. A novel colorimetric and off-on fluorescent chemosensor for Cr<sup>3+</sup> in aqueous solution and its application in live cell imaging. *Journal of Fluorescence* , 24: 119-127
- Li X H , Gao X H , Shi W , Ma H M. 2014b. Design strategies for water-soluble small molecular chromogenic and fluorogenic probes. *Chemical Reviews* , 114( 1) : 590-659
- Li Y , Dick W A , Tuovinen O H. 2004. Fluorescence microscopy for visualization of soil microorganisms-A review. *Biology and Fertility of Soils* , 39( 5) : 301-311
- Lichtman J W , Conchello J A. 2005. Fluorescence microscopy. *Nature Methods* , 2( 12) : 910-919
- Lin D , Ma W T , Jin Z X , Wang Y X , Huang Q Y , Cai P. 2016. Interactions of EPS with soil minerals: A combination study by ITC and CLSM. *Colloids and Surfaces B: Biointerfaces* , 138: 10-16
- Liu C , Huang S S , Yao H R , He S , Lu Y , Zhao L C , Zeng X S. 2014a. Preparation of fluorescein-based chemosensors and their sensing behaviors toward silver ions. *RSC Advances* , 4( 31) : 16109-16114
- Liu J J , Liu C , He W. 2013a. Fluorophores and their applications as molecular probes in living cells. *Current Organic Chemistry* , 17( 6) : 564-579
- Liu L J , Guo P , Chai L , Shi Q , Xu B H , Yuan J P , Wang X G , Shi X F , Zhang W Q. 2014b. Fluorescent and colorimetric detection of pH by a rhodamine-based probe. *Sensors and Actuators B: Chemical* , 194: 498-502
- Liu W H , Psaltis D , Barbastathis G. 2002. Real-time spectral imaging in three spatial dimensions. *Optics Letters* , 27( 10) : 854-856
- Liu W Y , Shen S L , Li H Y , Miao J Y , Zhao B X. 2013b. Fluorescence turn-on chemodosimeter for rapid detection of mercury ( II) ions in aqueous solution and blood from mice with toxicosis. *Analytica Chimica Acta* , 791: 65-71
- Liu X G , Yang L , Long Q , Weaver D , Hajnóczky G. 2017. Choosing proper fluorescent dyes , proteins , and imaging techniques to study mitochondrial dynamics in mammalian cells. *Biophysics Reports* , 3( 4-6) : 64-72
- Liu Y , Tang Y H , Barashkov N N , Irgibaeva I S , Lam J W Y , Hu R R , Birimzhanova D , Yu Y , Tang B Z. 2010. Fluorescent chemosensor for detection and quantitation of carbon dioxide gas. *Journal of the American Chemical Society* , 132( 40) : 13951-13953

- Lodeiro C, Capelo J L, Mejuto J C, Oliveira E, Santos H M, Pedras B, Nuñez C. 2010. Light and colour as analytical detection tools: A journey into the periodic table using polyamines to bio-inspired systems as chemosensors. *Chemical Society Reviews*, 39(8): 2948–2976
- Lou Z R, Li P, Han K L. 2015. Redox-responsive fluorescent probes with different design strategies. *Accounts of Chemical Research*, 48(5): 1358–1368
- Lukinavičius G, Reymond L, Umezawa K, Sallin O, D'Este E, Göttfert F, Ta H S, Hell S W, Urano Y, Johnsson K. 2016. Fluorogenic probes for multicolor imaging in living cells. *Journal of the American Chemical Society*, 138(30): 9365–9368
- Lv H S, Huang S Y, Zhao B X, Miao J Y. 2013a. A new rhodamine B-based lysosomal pH fluorescent indicator. *Analytica Chimica Acta*, 788: 177–182
- Lv H S, Liu J, Zhao J, Zhao B X, Miao J Y. 2013b. Highly selective and sensitive pH-responsive fluorescent probe in living HeLa and HUVEC cells. *Sensors and Actuators B: Chemical*, 177: 956–963
- Ma P Y, Liang F H, Wang D, Yang Q Q, Yang Z Q, Gao D J, Yu Y, Song D Q, Wang X H. 2015. A novel fluorescence and surface-enhanced Raman scattering dual-signal probe for pH sensing based on Rhodamine derivative. *Dyes and Pigments*, 122: 224–230
- Mahapatra A K, Manna S K, Maiti K, Maji R, Mukhopadhyay C D, Sarkar D, Mondal T K. 2014. Imino-phenolic-azodye appended rhodamine as a primary fluorescence "off-on" chemosensor for tin ( $\text{Sn}^{4+}$ ) in solution and in RAW cells and the recognition of sulphide by [AR-Sn]. *RSC Advances*, 4(69): 36615–36622
- Mahapatra A K, Manna S K, Maiti K, Mondal S, Maji R, Mandal D, Mandal S, Uddin M R, Goswami S, Quah C K, Fun H K. 2015. An azodye-rhodamine-based fluorescent and colorimetric probe specific for the detection of  $\text{Pd}^{2+}$  in aqueous ethanolic solution: Synthesis, XRD characterization, computational studies and imaging in live cells. *Analyst*, 140(4): 1229–1236
- Malide D, Métails J Y, Dunbar C E. 2014. *In vivo* clonal tracking of hematopoietic stem and progenitor cells marked by five fluorescent proteins using confocal and multiphoton microscopy. *Journal of Visualized Experiments*, (90): e51669
- Marks K M, Nolan G P. 2006. Chemical labeling strategies for cell biology. *Nature Methods*, 3(8): 591–596
- Marras S A E. 2006. Selection of fluorophore and quencher pairs for fluorescent nucleic acid hybridization probes. In: Didenko V V, ed. *Fluorescent Energy Transfer Nucleic Acid Probes: Designs and Protocols*. Totowa: Humana Press, 3–16
- Martin J P S, Martin S S. 2018. Exquisite preservation of a widespread filamentous microorganism in French Cretaceous ambers: Crucial for revising a controversial fossil. *Comptes Rendus Palevol*, 17(7): 415–434
- Maruo M, Inagawa H, Toratani Y, Kondo T, Matsushita M, Fujiyoshi S. 2014. Three-dimensional laser-scanning confocal reflecting microscope for multicolor single-molecule imaging at 1.5 K. *Chemical Physics Letters*, 591: 233–236
- Matruglio R, Horn H, Wagner M. 2014. Assessment and interpretation of the internal structure of biofilm streamers by combination of imaging techniques on two scales. *Journal of Advanced Microscopy Research*, 9(2): 79–85
- McLean J S, Ona O N, Majors P D. 2008. Correlated biofilm imaging, transport and metabolism measurements via combined nuclear magnetic resonance and confocal microscopy. *The ISME Journal*, 2(2): 121–131
- McRae R, Bagchi P, Sumalekshmy S, Fahmi C J. 2009. In situ imaging of metals in cells and tissues. *Chemical Reviews*, 109(10): 4780–4827
- Megías D, Marrero, Del Peso B M, García M Á, Bravo-Cordero J J, García-Grande A, Santos A, Montoya M C. 2009. Novel lambda FRET spectral confocal microscopy imaging method. *Microscopy Research and Technique*, 72(1): 1–11
- Meijering E, Cappellen G. 2007. Quantitative biological image analysis. In: Shorte S L, Frischknecht F, eds. *Imaging Cellular and Molecular Biological Functions*. Berlin: Springer, 45–70
- Milferstedt K, Pons M N, Morgenroth E. 2007. Texture analysis of spatial biofilm development. *Water Science and Technology*, 55(8–9): 481–488
- Milferstedt K, Pons M N, Morgenroth E. 2009. Analyzing characteristic length scales in biofilm structures. *Biotechnology and Bioengineering*, 102(2): 368–379
- Moßhammer M, Strobl M, Kühl M, Klimant I, Borisov S M, Koren K. 2016. Design and application of an optical sensor for simultaneous imaging of pH and dissolved  $\text{O}_2$  with low cross-talk. *ACS Sensors*, 1(6): 681–687
- Naber A, Plaschke M, Rothe J, Hofmann H, Fanghänel T. 2006. Scanning transmission X-ray and laser scanning luminescence microscopy of the carboxyl group and Eu(III) distribution in humic acid aggregates. *Journal of Electron Spectroscopy and Related Phenomena*, 153(3): 71–74
- Nanchaiah Y V, Wattiau P, Wuertz S, Bathe S, Mohan S V, Wilderer P A, Hausner M. 2003. Dual labeling of *Pseudomonas putida* with fluorescent proteins for in situ monitoring of conjugal transfer of the TOL plasmid. *Applied and Environmental Microbiology*, 69(8): 4846–4852
- Nedergaard M, Desai S, Pulsinelli W. 1990. Dicarboxy-dichlorofluorescein: A new fluorescent probe for measuring acidic intracellular pH. *Analytical Biochemistry*, 187(1): 109–114
- Neher R, Neher E. 2004. Optimizing imaging parameters for the separation of multiple labels in a fluorescence image. *Journal of microscopy*, 213(1): 46–62
- Neu T R, Lawrence J R. 2014a. Advanced techniques for in situ analysis of the biofilm matrix (structure, composition, dynamics) by means of laser scanning microscopy. In: Donelli G, ed. *Microbial Biofilms: Methods and Protocols*. New York: Humana Press, 43–64
- Neu T R, Lawrence J R. 2014b. Investigation of microbial biofilm structure by laser scanning microscopy. In: Muffler K, Ulber R, eds. *Productive Biofilms*. Berlin: Springer, 1–51
- Neu T R, Lawrence J R. 2014c. Protocol for laser scanning microscopy of microorganisms on hydrocarbons. In: McGenity T J, Timmis K N, Nogales B, eds. *Hydrocarbon and Lipid Microbiology Protocols*. Berlin: Springer, 1–19
- Neu T R, Lawrence J R. 2015. Innovative techniques, sensors, and approaches for imaging biofilms at different scales. *Trends in Microbiol-*

- ogy, 23(4): 233–242
- Nguyen T, Francis M B. 2003. Practical synthetic route to functionalized rhodamine dyes. *Organic Letters*, 5(18): 3245–3248
- Nix T, Feist-Burkhardt S. 2003. New methods applied to the microstructure analysis of Messel oil shale: Confocal Laser Scanning Microscopy (CLSM) and Environmental Scanning Electron Microscopy (ESEM). *Geological Magazine*, 140(4): 469–478
- Nosyk O, Ter Haseborg E, Metzger U, Frimmel F H. 2008. A standardized pre-treatment method of biofilm flocs for fluorescence microscopic characterization. *Journal of Microbiological Methods*, 75(3): 449–456
- Nudelman S, Ouimette D R. 1992–04–28. Multi-dimensional multi-spectral imaging system: US, 5109276
- Obare S O, De C, Guo W, Haywood T L, Samuels T A, Adams C P, Masika N O, Murray D H, Anderson G A, Campbell K, Fletcher K. 2010. Fluorescent chemosensors for toxic organophosphorus pesticides: A review. *Sensors*, 10(7): 7018–7043
- Obst M, Schmid G. 2014. 3D chemical mapping: Application of scanning transmission (soft) X-ray Microscopy (STXM) in combination with angle-scan tomography in Bio-, Geo-, and environmental sciences. In: Kuo J, ed. *Electron Microscopy*. Totowa: Humana Press, 757–781
- Oehler D Z, Cady S L. 2014. Biogenicity and syngeneity of organic matter in ancient sedimentary rocks: Recent advances in the search for evidence of past life. *Challenges*, 5(2): 260–283
- Ogawa M, Tani K, Ochiai A, Yamaguchi N, Nasu M. 2005. Multicolour digital image analysis system for identification of bacteria and concurrent assessment of their respiratory activity. *Journal of Applied Microbiology*, 98(5): 1101–1106
- Okumoto S, Jones A, Frommer W B. 2012. Quantitative imaging with fluorescent biosensors. *Annual Review of Plant Biology*, 63: 663–706
- Ono M, Murakami T, Kudo A, Isshiki M, Sawada H, Segawa A. 2001. Quantitative comparison of anti-fading mounting media for confocal laser scanning microscopy. *Journal of Histochemistry & Cytochemistry*, 49(3): 305–311
- Ozdemir M. 2016. A selective fluorescent ‘turn-on’ sensor for recognition of Zn<sup>2+</sup> in aqueous media. *Spectrochimica Acta Part A: Molecular and Biomolecular Spectroscopy*, 161: 115–121
- Paddock S W. 2000. Principles and practices of laser scanning confocal microscopy. *Molecular Biotechnology*, 16(2): 127–149
- Paddock S W, Eliceiri K W. 2014. Laser scanning confocal microscopy: History, applications, and related optical sectioning techniques. In: Paddock S W, ed. *Confocal Microscopy: Methods and Protocols*. New York: Springer, 9–47
- Pan Y H, Hu L, Zhao T. 2019. Applications of chemical imaging techniques in paleontology. *National Science Review*, 6(5): 1040–1053
- Parker K J, Kumar S, Pearce D A, Sutherland A J. 2005. Design, synthesis and evaluation of a fluorescent peptidyl sensor for the selective recognition of arsenite. *Tetrahedron Letters*, 46(41): 7043–7045
- Pasteris J D, Freeman J J, Goffredi S K, Buck K R. 2001. Raman spectroscopic and laser scanning confocal microscopic analysis of sulfur in living sulfur-precipitating marine bacteria. *Chemical Geology*, 180(1–4): 3–18
- Pawley J B. 2006. *Handbook of biological confocal microscopy*. Boston: Springer
- Pepperkok R, Ellenberg J. 2006. High-throughput fluorescence microscopy for systems biology. *Nature Reviews Molecular Cell Biology*, 7(9): 690–696
- Perkovic M, Kunz M, Endesfelder U, Bunse S, Wigge C, Yu Z, Hodi-irnav V V, Scheffer M P, Seybert A, Malkusch S, Schuman E M, Heilemann M, Frangakis A S. 2014. Correlative light- and electron microscopy with chemical tags. *Journal of Structural Biology*, 186(2): 205–213
- Petrat F, De Groot H, Rauen U. 2000. Determination of the chelatable iron pool of single intact cells by laser scanning microscopy. *Archives of Biochemistry and Biophysics*, 376(1): 74–81
- Pluth M D, Tomat E, Lippard S J. 2011. Biochemistry of mobile zinc and nitric oxide revealed by fluorescent sensors. *Annual Review of Biochemistry*, 80: 333–355
- Posth N R, Huelin S, Konhauser K O, Kappler A. 2010. Size, density and composition of cell-mineral aggregates formed during anoxygenic phototrophic Fe(II) oxidation: Impact on modern and ancient environments. *Geochimica et Cosmochimica Acta*, 74(12): 3476–3493
- Prow T W, Kotov N A, Lvov Y M, Rijnbrand R, Leary J F. 2004. Nanoparticles, molecular biosensors, and multispectral confocal microscopy. *Journal of Molecular Histology*, 35(6): 555–564
- Qian X H, Xiao Y, Xu Y F, Guo X F, Qian J H, Zhu W P. 2010. "Alive" dyes as fluorescent sensors: Fluorophore, mechanism, receptor and images in living cells. *Chemical Communications*, 46(35): 6418–6436
- Quang D T, Kim J S. 2010. Fluoro- and chromogenic chemodosimeters for heavy metal ion detection in solution and biospecimens. *Chemical Reviews*, 110(10): 6280–6301
- Que E L, Domaille D W, Chang C J. 2008. Metals in neurobiology: Probing their chemistry and biology with molecular imaging. *Chemical Reviews*, 108(5): 1517–1549
- Rabut G, Ellenberg J. 2004. Automatic real-time three-dimensional cell tracking by fluorescence microscopy. *Journal of Microscopy*, 216(2): 131–137
- Rasheed T, Li C L, Bilal M, Yu C Y, Iqbal H M N. 2018. Potentially toxic elements and environmentally-related pollutants recognition using colorimetric and ratiometric fluorescent probes. *Science of the Total Environment*, 640–641: 174–193
- Resch-Genger U, Grabolle M, Cavaliere-Jaricot S, Nitschke R, Nann T. 2008. Quantum dots versus organic dyes as fluorescent labels. *Nature Methods*, 5(9): 763–775
- Roudeau S, Carmona A, Perrin L, Ortega R. 2014. Correlative organelle fluorescence microscopy and synchrotron X-ray chemical element imaging in single cells. *Analytical and Bioanalytical Chemistry*, 406(27): 6979–6991
- Rudd N C, Cannan S, Bitziou E, Ciani I, Whitworth A L, Unwin P R. 2005. Fluorescence confocal laser scanning microscopy as a probe of pH gradients in electrode reactions and surface activity. *Analytical Chemistry*, 77(19): 6205–6217
- Sahana S, Bose S, Mukhopadhyay S K, Bharadwaj P K. 2016. A highly selective and sensitive turn-on fluorescence chemosensor based on a rhodamine-adenine conjugate for Al<sup>3+</sup> in aqueous medium:

- Bioimaging and DFT studies. *Journal of Luminescence*, 169: 334–341
- Sauer M. 2003. Single-molecule-sensitive fluorescent sensors based on photoinduced intramolecular charge transfer. *Angewandte Chemie International Edition*, 42(16): 1790–1793
- Sauvé S, Hendershot W, Allen H E. 2000. Solid-solution partitioning of metals in contaminated soils: Dependence on pH, total metal burden, and organic matter. *Environmental Science & Technology*, 34(7): 1125–1131
- Schäferling M. 2012. The art of fluorescence imaging with chemical sensors. *Angewandte Chemie International Edition*, 51(15): 3532–3554
- Schlafer S, Meyer R L. 2017. Confocal microscopy imaging of the biofilm matrix. *Journal of Microbiological Methods*, 138: 50–59
- Schmid G, Zeitvogel F, Hao L, Ingino P, Floetenmeyer M, Stierhof Y D, Schroeppel B, Burkhardt C J, Kappler A, Obst M. 2014. 3-D analysis of bacterial cell-(iron) mineral aggregates formed during Fe(II) oxidation by the nitrate-reducing *Acidovorax* sp. strain BoFeN1 using complementary microscopy tomography approaches. *Geobiology*, 12(4): 340–361
- Schneider A F L, Hackenberger C P R. 2017. Fluorescent labelling in living cells. *Current Opinion in Biotechnology*, 48: 61–68
- Schopf J W, Tripathi A B, Kudryavtsev A B. 2006. Three-dimensional confocal optical imagery of precambrian microscopic organisms. *Astrobiology*, 6(1): 1–16
- Schopf J W, Kudryavtsev A B. 2009. Confocal laser scanning microscopy and Raman imagery of ancient microscopic fossils. *Precambrian Research*, 173(1–4): 39–49
- Schopf J W, Kudryavtsev A B, Sergeev V N. 2010a. Confocal laser scanning microscopy and raman imagery of the late neoproterozoic chichkan microbiota of south Kazakhstan. *Journal of Paleontology*, 84(3): 402–416
- Schopf J W, Kudryavtsev A B, Sugitani K, Walter M R. 2010b. Precambrian microbe-like pseudofossils: A promising solution to the problem. *Precambrian Research*, 179(1–4): 191–205
- Schopf J W. 2011. The paleobiological record of photosynthesis. *Photosynthesis Research*, 107: 87–101
- Schopf J W. 2012. The fossil record of cyanobacteria. In: Whitton B A, ed. *Ecology of Cyanobacteria II: Their Diversity in Space and Time*. Dordrecht: Springer, 15–36
- Schopf J W, Kudryavtsev A B. 2012. Biogenicity of Earth's earliest fossils: A resolution of the controversy. *Gondwana Research*, 22(3–4): 761–771
- Schopf J W, Calça C P, Garcia A K, Kudryavtsev A B, Souza P A, Félix C M, Fairchild T R. 2016. *In situ* confocal laser scanning microscopy and Raman spectroscopy of bisaccate pollen from the Irati Subgroup (Permian, Paraná Basin, Brazil): Comparison with acid-macerated specimens. *Review of Palaeobotany and Palynology*, 233: 169–175
- Schopf J W, Kudryavtsev A B, Osterhout J T, Williford K H, Kitajima K, Valley J W, Sugitani K. 2017. An anaerobic ~3400 Ma shallow-water microbial consortium: Presumptive evidence of Earth's Paleoproterozoic anoxic atmosphere. *Precambrian Research*, 299: 309–318
- Schopf J W, Garcia A K. 2019. Application of the apatite oxygen paleo-barometer (AOP) across the Neoproterozoic-Cambrian transition. *Precambrian Research*, 105404, <https://doi.org/10.1016/j.precamres.2019.105404>
- Schramm A, De Beer D, Gieseke A, Amann R. 2000. Microenvironments and distribution of nitrifying bacteria in a membrane-bound biofilm. *Environmental Microbiology*, 2(6): 680–686
- Schutting S, Klimant I, De Beer D, Borisov S M. 2014. New highly fluorescent pH indicator for ratiometric RGB imaging of pCO<sub>2</sub>. *Methods and Applications in Fluorescence*, 2(2): 024001
- Scott A C. 1989. Geological applications of laser scanning microscopy. *Microscopy and Analysis*, 1989, 10: 17–19
- Scriven D R L, Lynch R M, Moore E D W. 2008. Image acquisition for colocalization using optical microscopy. *American Journal of Physiology-Cell Physiology*, 294(5): C1119–C1122
- Shah S M, Crawshaw J P, Boek E S. 2017. Three-dimensional imaging of porous media using confocal laser scanning microscopy. *Journal of Microscopy*, 265(2): 261–271
- Shaner N C, Steinbach P A, Tsien R Y. 2005. A guide to choosing fluorescent proteins. *Nature Methods*, 2(12): 905–909
- She M Y, Yang Z, Yin B, Zhang J, Gu J, Yin W T, Li J L, Zhao G F, Shi Z. 2012. A novel rhodamine-based fluorescent and colorimetric “off-on” chemosensor and investigation of the recognizing behavior towards Fe<sup>3+</sup>. *Dyes and Pigments*, 92(3): 1337–1343
- Shi W, Sun S N, Li X H, Ma H M. 2010. Imaging different interactions of mercury and silver with live cells by a designed fluorescence probe rhodamine B selenolactone. *Inorganic Chemistry*, 49(3): 1206–1210
- Shiraishi F, Reimer A, Bissett A, De Beer D, Arp G. 2008. Microbial effects on biofilm calcification, ambient water chemistry and stable isotope records in a highly supersaturated setting (Westerhöfer Bach, Germany). *Palaeogeography, Palaeoclimatology, Palaeoecology*, 262(1–2): 91–106
- Shumi W, Lim J, Nam S W, Kim S H, Cho K S, Yoon J, Park S. 2009. Fluorescence imaging of the spatial distribution of ferric ions over biofilms formed by *Streptococcus mutans* under microfluidic conditions. *Biochip Journal*, 3: 119–124
- Simpson A W M. 2013. Fluorescent measurement of [Ca<sup>2+</sup>]<sub>i</sub>: Basic practical considerations. In: Lambert D G, Rainbow R D, eds. *Calcium Signaling Protocols*. Totowa: Humana Press, 3–36
- Sinclair M B, Haaland D M, Timlin J A, Jones H D T. 2006. Hyperspectral confocal microscope. *Applied Optics*, 45(24): 6283–6291
- Slavík J. 1983. Intracellular pH topography: Determination by a fluorescent probe. *FEBS Letters*, 156(2): 227–230
- Solé A, Diestra E, Esteve I. 2009. Confocal laser scanning microscopy image analysis for cyanobacterial biomass determined at microscale level in different microbial mats. *Microbial Ecology*, 57(4): 649–656
- Spear R N, Cullen D, Andrews J H. 1999. Fluorescent labels, confocal microscopy, and quantitative image analysis in study of fungal biology. *Methods in Enzymology*, 307: 607–623
- Staudt C, Horn H, Hempel D C, Neu T R. 2004. Volumetric measurements of bacterial cells and extracellular polymeric substance glycoconjugates in biofilms. *Biotechnology and Bioengineering*, 88(5): 585–592

- Stennett E M S , Ciuba M A , Levitus M. 2014. Photophysical processes in single molecule organic fluorescent probes. *Chemical Society Reviews* , 43( 4) : 1057–1075
- Stephanopoulos N , Francis M B. 2011. Choosing an effective protein bioconjugation strategy. *Nature Chemical Biology* , 7( 12) : 876–884
- Stephens D J , Allan V J. 2003. Light microscopy techniques for live cell imaging. *Science* , 300( 5616) : 82–86
- Stich M I J , Schaeferling M , Wolfbeis O S. 2009. Multicolor fluorescent and permeation-selective microbeads enable simultaneous sensing of pH , oxygen , and temperature. *Advanced Materials* , 21( 21) : 2216–2220
- Stich M I J , Fischer L H , Wolfbeis O S. 2010. Multiple fluorescent chemical sensing and imaging. *Chemical Society Reviews* , 39( 8) : 3102–3114
- Studer V , Bobin J , Chahid M , Mousavi H S , Candes E , Dahan M. 2012. Compressive fluorescence microscopy for biological and hyperspectral imaging. *Proceedings of the National Academy of Sciences of the United States of America* , 109( 26) : E1679–E1687
- Sun H H , Scharff-Poulsen A M , Gu H , Almdal K. 2006. Synthesis and characterization of ratiometric , pH sensing nanoparticles with covalently attached fluorescent dyes. *Chemistry of Materials* , 18( 15) : 3381–3384
- Sun Y Q , Liu J , Lv X , Liu Y L , Zhao Y , Guo W. 2012. Rhodamine-inspired far-red to near-infrared dyes and their application as fluorescence probes. *Angewandte Chemie International Edition* , 51( 31) : 7634–7636
- Suzuki T , Matsuzaki T , Takata K. 1998. Fluorescence counter-staining of cell nuclear DNA for multi-color laser confocal microscopy. *Acta Histochemica et Cytochemica* , 31( 4) : 297–301
- Swanner E D , Wu W F , Hao L K , Wüstner M L , Obst M , Moran D M , McIlvin M R , Saito M A , Kappler A. 2015a. Physiology , Fe( II) oxidation , and Fe mineral formation by a marine planktonic cyanobacterium grown under ferruginous conditions. *Frontiers in Earth Science* , 3: 60
- Swanner E D , Wu W F , Schoenberg R , Byrne J , Michel F M , Pan Y X , Kappler A. 2015b. Fractionation of Fe isotopes during Fe( II) oxidation by a marine photofeotroph is controlled by the formation of organic Fe-complexes and colloidal Fe fractions. *Geochimica et Cosmochimica Acta* , 165: 44–61
- Swanner E D , Bayer T , Wu W , Hao L , Obst M , Sundman A , Byrne J M , Michel F M , Kleinhans I C , Kappler A , Schoenberg R. 2017. Iron isotope fractionation during Fe( II) oxidation mediated by the oxygen-producing marine cyanobacterium *Synechococcus* PCC 7002. *Environmental Science & Technology* , 51( 9) : 4897–4906
- Tanaka K , Miura T , Umezawa N , Urano Y , Kikuchi K , Higuchi T , Nagano T. 2001. Rational design of fluorescein-based fluorescence probes. Mechanism-based design of a maximum fluorescence probe for singlet oxygen. *Journal of the American Chemical Society* , 123( 11) : 2530–2536
- Tashyreva D , Elster J , Billi D. 2013. A novel staining protocol for multiparameter assessment of cell heterogeneity in *Phormidium* populations (Cyanobacteria) employing fluorescent dyes. *PLoS One* , 8( 2) : e55283
- Tearney G J , Webb R H , Bouma B E. 1998. Spectrally encoded confocal microscopy. *Optics Letters* , 23( 15) : 1152–1154
- Terai T , Nagano T. 2008. Fluorescent probes for bioimaging applications. *Current Opinion in Chemical Biology* , 12( 5) : 515–521
- Tewari V C. 2011. Stromatolites , organic-walled microorganisms , laser raman spectroscopy , and confocal laser scanning microscopy of the meso- neoproterozoic buxa formation , ranjit window , sikkim lesser himalaya , NE India. In: Tewari V , Seckbach J , eds. *STROMATOLITES: Interaction of Microbes with Sediments*. Dordrecht: Springer , 495–522
- Thivierge C , Han J Y , Jenkins R M , Burgess K. 2011. Fluorescent proton sensors based on energy transfer. *The Journal of Organic Chemistry* , 76( 13) : 5219–5228
- Thompson R B. 2005. Studying zinc biology with fluorescence: Ain' t we got fun? *Current Opinion in Chemical Biology* , 9( 5) : 526–532
- Tolker-Nielsen T , Molin S. 2000. Spatial organization of microbial biofilm communities. *Microbial Ecology* , 40( 2) : 75–84
- Tomat E , Lippard S J. 2010. Imaging mobile zinc in biology. *Current Opinion in Chemical Biology* , 14( 2) : 225–230
- Tratnyek P G , Reiloff T E , Lemon A W , Scherer M M , Balko B A , Feik L M , Henegar B D. 2001. Visualizing redox chemistry: Probing environmental oxidation-reduction reactions with indicator dyes. *The Chemical Educator* , 6( 3) : 172–179
- Trevors J T. 2003. Fluorescent probes for bacterial cytoplasmic membrane research. *Journal of Biochemical and Biophysical Methods* , 57( 2) : 87–103
- Tsien R Y , Poenie M. 1986. Fluorescence ratio imaging: A new window into intracellular ionic signaling. *Trends in Biochemical Sciences* , 11( 11) : 450–455
- Turillazzi E , Karch S B , Neri M , Pomara C , Riezzo I , Fineschi V. 2008. Confocal laser scanning microscopy. Using new technology to answer old questions in forensic investigations. *International Journal of Legal Medicine* , 122( 2) : 173–177
- Ueno T , Nagano T. 2011. Fluorescent probes for sensing and imaging. *Nature Methods* , 8( 8) : 642–645
- Ueshima M , Ginn B R , Haack E A , Szymanowski J E S , Fein J B. 2008. Cd adsorption onto *Pseudomonas putida* in the presence and absence of extracellular polymeric substances. *Geochimica et Cosmochimica Acta* , 72( 24) : 5885–5895
- Unciti-Broceta A , Yusop M R , Richardson P R , Walton J G A , Bradley M. 2009. A fluorescein-derived anthocyanidin-inspired pH sensor. *Tetrahedron Letters* , 50( 35) : 3713–3715
- Urano Y , Asanuma D , Hama Y , Koyama Y , Barrett T , Kamiya M , Nagano T , Watanabe T , Hasegawa A , Choyke P L , Kobayashi H. 2009. Selective molecular imaging of viable cancer cells with pH-activatable fluorescence probes. *Nature Medicine* , 15: 104–109
- Valle E R , Henderson G , Janssen P H , Cox F , Alexander T W , McAllister T A. 2015. Considerations in the use of fluorescence in situ hybridization ( FISH) and confocal laser scanning microscopy to characterize rumen methanogens and define their spatial distributions. *Canadian Journal of Microbiology* , 61( 4) : 417–428
- Valm A M , Oldenbourg R , Borisy G G. 2016. Multiplexed spectral imaging of 120 different fluorescent labels. *PLoS One* , 11( 7) : e0158495
- Vendrell M , Zhai D T , Er J C , Chang Y T. 2012. Combinatorial strate-

- gies in fluorescent probe development. *Chemical Reviews*, 112(8): 4391–4420
- Vukojević V, Heidkamp M, Ming Y, Johansson B, Terenius L, Rigler R. 2008. Quantitative single-molecule imaging by confocal laser scanning microscopy. *Proceedings of the National Academy of Sciences of the United States of America*, 105(47): 18176–18181
- Wacey D. 2009. *Early life on earth: A practical guide*. Dordrecht: Springer
- Waggoner A, Moerner W E, Bruchez M. 2013. Fluorescent probes and digital imaging: Where we are and where we're going. *Science*, 340(6137): 1247
- Wang J, Karpus J, Zhao B S, Luo Z, Chen P R, He C. 2012. A selective fluorescent probe for carbon monoxide imaging in living cells. *Angewandte Chemie*, 124(38): 9790–9794
- Wang X D, Wolfbeis O S, Meier R J. 2013. Luminescent probes and sensors for temperature. *Chemical Society Reviews*, 42(19): 7834–7869
- Warren L A, Haack E A. 2001. Biogeochemical controls on metal behaviour in freshwater environments. *Earth-Science Reviews*, 54(4): 261–320
- Wessel A K, Hmelo L, Parsek M R, Whiteley M. 2013. Going local: Technologies for exploring bacterial microenvironments. *Nature Reviews Microbiology*, 11(5): 337–348
- White A G, Gray B D, Pak K Y, Smith B D. 2012. Deep-red fluorescent imaging probe for bacteria. *Bioorganic & Medicinal Chemistry Letters*, 22(8): 2833–2836
- Wouterlood F G. 2014. Analysis of brain projection systems using third-generation neuroanatomical tracers and multiple fluorescence laser scanning microscopy. In: Bakota L, Brandt R, eds. *Laser Scanning Microscopy and Quantitative Image Analysis of Neuronal Tissue*. New York: Springer, 51–82
- Wu C, Bian Q N, Zhang B G, Cai X, Zhang S D, Zheng H, Yang S Y, Jiang Y B. 2012. Ring expansion of spiro-thiolactam in rhodamine scaffold: Switching the recognition preference by adding one atom. *Organic Letters*, 14(16): 4198–4201
- Wu J, Rajwa B, Filmer D L, Hoffmann C M, Yuan B, Chiang C, Sturgis J, Robinson J P. 2003. Automated quantification and reconstruction of collagen matrix from 3D confocal datasets. *Journal of Microscopy*, 210(2): 158–165
- Wu W F, Swanner E D, Hao L K, Zeitvogel F, Obst M, Pan Y X, Kappler A. 2014. Characterization of the physiology and cell-mineral interactions of the marine anoxygenic phototrophic Fe(II) oxidizer *Rhodovulum iodolum*-implications for Precambrian Fe(II) oxidation. *FEMS Microbiology Ecology*, 88(3): 503–515
- Wuertz S, Müller E, Spaeth R, Pfeleiderer P, Flemming H C. 2000. Detection of heavy metals in bacterial biofilms and microbial flocs with the fluorescent complexing agent Newport Green. *Journal of Industrial Microbiology and Biotechnology*, 24(2): 116–123
- Wysocki L M, Grimm J B, Tkachuk A N, Brown T A, Betzig E, Lavis L D. 2011. Facile and general synthesis of photoactivatable xanthenes dyes. *Angewandte Chemie International Edition*, 50(47): 11206–11209
- Xie X M, Borjiigin T, Zhang Q Z, Zhang Z R, Qin J Z, Bian L Z, Volkman J K. 2015. Intact microbial fossils in the Permian Lucaogou Formation oil shale, Junggar Basin, NW China. *International Journal of Coal Geology*, 146: 166–178
- Xiong X Q, Song F L, Wang J Y, Zhang Y K, Xue Y Y, Sun L L, Jiang N, Gao P, Tian L, Peng X J. 2014. Thermally activated delayed fluorescence of fluorescein derivative for time-resolved and confocal fluorescence imaging. *Journal of the American Chemical Society*, 136(27): 9590–9597
- Xu K H, Chen H C, Tian J W, Ding B Y, Xie Y X, Qiang M M, Tang B. 2011a. A near-infrared reversible fluorescent probe for peroxynitrite and imaging of redox cycles in living cells. *Chemical Communications*, 47(33): 9468–9470
- Xu L, Xu Y F, Zhu W P, Zeng B B, Yang C M, Wu B, Qian X H. 2011b. Versatile trifunctional chemosensor of rhodamine derivative for Zn<sup>2+</sup>, Cu<sup>2+</sup> and His/Cys in aqueous solution and living cells. *Organic & Biomolecular Chemistry*, 9(24): 8284–8287
- Xu L, Xu Y F, Zhu W P, Sun X L, Xu Z, Qian X H. 2012. Modulating the selectivity by switching sensing media: A bifunctional chemosensor selectivity for Cd<sup>2+</sup> and Pb<sup>2+</sup> in different aqueous solutions. *RSC Advances*, 2(15): 6323–6328
- Xu L Q, Zhang B, Sun M, Hong L, Neoh K G, Kang E T, Fu G D. 2013. CO<sub>2</sub>-triggered fluorescence "turn-on" response of perylene diimide-containing poly(*N,N*-dimethylaminoethyl methacrylate). *Journal of Materials Chemistry A*, 1(4): 1207–1212
- Xu Z C, Han S J, Lee C, Yoon J, Spring D R. 2010. Development of off-on fluorescent probes for heavy and transition metal ions. *Chemical Communications*, 46(10): 1679–1681
- Xue Z W, Chen M L, Chen J M, Han J H, Han S F. 2014. A rhodamine-benzimidazole based sensor for selective imaging of acidic pH. *RSC Advances*, 4(1): 374–378
- Yang L, Hu Y F, Liu Y, Zhang J D, Ulstrup J, Molin S. 2011a. Distinct roles of extracellular polymeric substances in *Pseudomonas aeruginosa* biofilm development. *Environmental Microbiology*, 13(7): 1705–1717
- Yang Q, Zou J R, Chirumarry S, Huo C, Tang L L, Zhang F, Xiang Y, Zuo H, Shin D S, Peng X. 2016. A new rhodamine B-based fluorescent probe for pH detection and bioimaging under strong acidic conditions. *Bulletin of the Korean Chemical Society*, 37(9): 1453–1457
- Yang Y M, Zhao Q, Feng W, Li F Y. 2013. Luminescent chemodosimeters for bioimaging. *Chemical Reviews*, 113(1): 192–270
- Yang Y X, Gao W L, Sheng R L, Wang W L, Liu H, Yang W M, Zhang T Y, Zhang X T. 2011b. Rhodamine-based derivatives for Cu<sup>2+</sup> sensing: Spectroscopic studies, structure-recognition relationships and its test strips. *Spectrochimica Acta Part A: Molecular and Biomolecular Spectroscopy*, 81(1): 14–20
- Yang Z, She M Y, Ma S Y, Yin B, Liu P, Liu X R, Zhao S S, Li J L. 2017. Rhodamine based guanidinobenzimidazole functionalized fluorescent probe for tetravalent tin and its application in living cells imaging. *Sensors and Actuators B: Chemical*, 242: 872–879
- Yeung T, Touret N, Grinstead S. 2005. Quantitative fluorescence microscopy to probe intracellular microenvironments. *Current Opinion in Microbiology*, 8(3): 350–358
- Yin J, Hu Y, Yoon J. 2015. Fluorescent probes and bioimaging: Alkali metals, alkaline earth metals and pH. *Chemical Society Reviews*, 44

- (14): 4619-4644
- Yu G H, Tang Z, Xu Y C, Shen Q R. 2011a. Multiple fluorescence labeling and two dimensional FTIR  $-^{13}\text{C}$  NMR heterospectral correlation spectroscopy to characterize extracellular polymeric substances in biofilms produced during composting. *Environmental Science & Technology*, 45(21): 9224-9231
- Yu H B, Li G L, Zhang B, Zhang X F, Xiao Y, Wang J Q, Song Y T. 2016. A neutral pH probe of rhodamine derivatives inspired by effect of hydrogen bond on pKa and its organelle-targetable fluorescent imaging. *Dyes and Pigments*, 133: 93-99
- Yu M X, Shi M, Chen Z G, Li F Y, Li X X, Gao Y H, Xu J, Yang H, Zhou Z G, Yi T, Huang C H. 2008. Highly sensitive and fast responsive fluorescence turn-on chemodosimeter for  $\text{Cu}^{2+}$  and its application in live cell imaging. *Chemistry-A European Journal*, 14(23): 6892-6900
- Yu Y, Trouvé A, Chalmond B, Renaud O, Shorte S L. 2011b. Confocal bi-protocol: A new strategy for isotropic 3D live cell imaging. *Journal of Microscopy*, 242(1): 70-85
- Yuan B, Wang X H, Tang C Y, Li X F, Yu G H. 2015. In situ observation of the growth of biofouling layer in osmotic membrane bioreactors by multiple fluorescence labeling and confocal laser scanning microscopy. *Water Research*, 75: 188-200
- Yuan L, Lin W Y, Tan L, Zheng K B, Huang W M. 2013a. Lighting up carbon monoxide: Fluorescent probes for monitoring CO in living cells. *Angewandte Chemie International Edition*, 52(6): 1628-1630
- Yuan L, Lin W Y, Zheng K B, He L W, Huang W. 2013b. Far-red to near infrared analyte-responsive fluorescent probes based on organic fluorophore platforms for fluorescence imaging. *Chemical Society Reviews*, 42(2): 622-661
- Zeitvogel F, Burkhardt C J, Schroepel B, Schmid G, Ingino P, Obst M. 2017. Comparison of preparation methods of bacterial cell-mineral aggregates for SEM imaging and analysis using the model system of *Acidovorax* sp. BoFeN1. *Geomicrobiology Journal*, 34(4): 317-327
- Zhang D, Li M, Wang M, Wang J H, Yang X, Ye Y, Zhao Y F. 2013a. A rhodamine-phosphonate off-on fluorescent sensor for  $\text{Hg}^{2+}$  in natural water and its application in live cell imaging. *Sensors and Actuators B: Chemical*, 177: 997-1002
- Zhang J, Campbell R E, Ting A Y, Tsien R Y. 2002. Creating new fluorescent probes for cell biology. *Nature Reviews Molecular Cell Biology*, 3(12): 906-918
- Zhang J F, Zhou Y, Yoon J, Kim J S. 2011a. Recent progress in fluorescent and colorimetric chemosensors for detection of precious metal ions (silver, gold and platinum ions). *Chemical Society Reviews*, 40(7): 3416-3429
- Zhang L F, Zhao J L, Zeng X, Mu L, Jiang X K, Deng M, Zhang J X, Wei G. 2011b. Tuning with pH: The selectivity of a new rhodamine B derivative chemosensor for  $\text{Fe}^{3+}$  and  $\text{Cu}^{2+}$ . *Sensors and Actuators B: Chemical*, 160(1): 662-669
- Zhang P, Chen Y P, Qiu J H, Dai Y Z, Feng B. 2019a. Imaging the microprocesses in biofilm matrices. *Trends in Biotechnology*, 37(2): 214-226
- Zhang P, Feng B, Chen Y P, Dai Y Z, Guo J S. 2019b. *In situ* characterizations for EPS-involved microprocesses in biological wastewater treatment systems. *Critical Reviews in Environmental Science and Technology*, 49(11): 917-946
- Zhang W S, Tang B, Liu X, Liu Y Y, Xu K H, Ma J P, Tong L L, Yang G W. 2009. A highly sensitive acidic pH fluorescent probe and its application to HepG2 cells. *Analyst*, 134(2): 367-371
- Zhang X Q, Bishop P L. 2001. Spatial distribution of extracellular polymeric substances in biofilms. *Journal of Environmental Engineering*, 127(9): 850-856
- Zhang Y H, Hu B, Dai Y K, Yang H M, Huang W, Xue X J, Li F Z, Zhang X, Jiang C Y, Gao F, Chang J. 2013b. A new multichannel spectral imaging laser scanning confocal microscope. *Computational and Mathematical Methods in Medicine*, 2013, 2013: 890203
- Zhang Z, Zheng Y, Hang W, Yan X M, Zhao Y F. 2011c. Sensitive and selective off-on rhodamine hydrazide fluorescent chemosensor for hypochlorous acid detection and bioimaging. *Talanta*, 85(1): 779-786
- Zhao X X, Chen X P, Shen S L, Li D P, Zhou S, Zhou Z Q, Xiao Y H, Xi G, Miao J Y, Zhao B X. 2014. A novel pH probe based on a rhodamine-rhodamine platform. *RSC Advances*, 4(92): 50318-50324
- Zheng A F, Chen J L, Wu G H, Wu G L, Zhang Y G, Wei H P. 2009. A novel fluorescent distinguished probe for Cr(VI) in aqueous solution. *Spectrochimica Acta Part A: Molecular and Biomolecular Spectroscopy*, 74(1): 265-270
- Zhou Y, Xu Z C, Yoon J. 2011. Fluorescent and colorimetric chemosensors for detection of nucleotides, FAD and NADH: Highlighted research during 2004-2010. *Chemical Society Reviews*, 40(5): 2222-2235
- Zimmermann T, Rietdorf J, Pepperkok R. 2003. Spectral imaging and its applications in live cell microscopy. *FEBS Letters*, 546(1): 87-92
- Zimmermann T. 2005. Spectral imaging and linear unmixing in light microscopy. In: Rietdorf J, ed. *Microscopy Techniques*. Berlin: Springer, 245-265
- Zimmermann T, Marrison J, Hogg K, O'Toole P. 2014. Clearing up the signal: Spectral imaging and linear unmixing in fluorescence microscopy. In: Paddock S W, ed. *Confocal Microscopy*. New York: Springer, 129-148
- Zippel B, Neu T R. 2011. Characterization of glycoconjugates of extracellular polymeric substances in tufa-associated biofilms by using fluorescence lectin-binding Analysis. *Applied and Environmental Microbiology*, 77(2): 505-516
- Zou X S, Pan T T, Chen L, Tian Y Q, Zhang W W. 2017. Luminescence materials for pH and oxygen sensing in microbial cells-structures, optical properties, and biological applications. *Critical Reviews in Biotechnology*, 37(6): 723-738

(本文责任编辑: 龚超颖; 英文审校: 张兴春)



## 专栏作者简介



苏文,1962年生,中国科学院地质与地球物理研究所研究员,博士生导师。主要研究方向为名义上无水矿物/含水矿物中水/流体组分在高温高压条件下赋存特征、显微结构及矿物学实验。主持、参加并完成了多个国家自然科学基金重大项目、创新研究群体、

973项目、国家自然科学基金面上基金和部级项目研究工作。出版专著一部,发表论文83篇,其中以第一作者的身份发表论文31篇(27篇为SCI文章);曾获国家自然科学基金三等奖、安徽省科技进步二等奖和四等奖,被中国科学院授予2002年度优秀博士后荣誉称号、获得中国地质学会第一届优秀女地质科技工作者奖;与MICROPTICS合作,在布鲁克Vertex 70v真空型红外光谱仪上,搭建了一套适用于高压、高温测量的傅立叶变换红外显微系统的科学实验平台。



李秋立,1977年生,中国科学院地质与地球物理研究所研究员,博士生导师,现任离子探针实验室主任和化学地球动力学学科组组长。1998年毕业于西北大学地质系,2003年于中国科学技术大学获地球

化学博士学位,主要从事同位素地质年代学和地球化学的研究,研究生期间研发了微量金红石U-Pb定年方法,博士后期间建立了微量样品Rb-Sr等时线定年方法,近十余年来集中于离子探针微区测试技术,研发了10种以上副矿物微区原位U-Th-Pb年龄测试方法,为解决超碱性岩类、碳酸岩类、陨石、碎屑沉积岩、中低温变质岩、矿床等定年难题提供了有效定年手段。发表SCI论文180余篇,SCI引用5000余次,入选ESI高引用率名录。获得2008年安徽科学技术奖一等奖、2010年国家自然科学二等奖,2012年获首届国家优秀青年基金,2014年入选中组部“万人计划”青年拔尖人才,2014年获中国矿

物岩石地球化学学会“侯德封奖”,2017年获第十二届“中国科学院杰出青年”称号,2018年获Shen-Su Sun Award(孙贤鉢奖)。担任Canadian Journal of Earth Sciences和Mineralogy and Petrology国际SCI期刊Associate editor。



李金华,1979年生,中国科学院地质与地球物理研究所研究员,博士生导师,电子显微镜实验室主任。获2015年度国家自然科学基金“优秀青年科学基金”项目资助,是中国地球物理学会2015年“傅承

义青年科技奖”获得者。研究方向为“地球生物学”和“生物地磁学”,发表SCI论文70余篇。主持国家自然科学基金“重大项目课题、重点国际合作和面上项目(青年-面上连续资助)”等8项国家级项目。近年来,在学科交叉和技术研发领域开展了卓有成效的工作,推动古地磁学、微生物学、古生物学和地质学等领域的大幅度跨学科交叉,以微生物矿化和微化石识别为核心,深入探索微生物参与和微化石记录的地球与生命演化过程,从而把生命演化和地质演化这两条最重要的科学线交接了起来,在生物磁学和地球生物学领域做出了创新性的工作。另一方面,致力于推动纳米地球科学的学科发展和技术研发,组织了中国第一届“显微学与显微谱学及其在纳米地球科学中应用”研讨会,搭建了跨学科跨领域的显微学与显微谱学研究平台,研发了“荧光-电子显微镜联用”技术,首次在单细胞水平上实现了微生物种类鉴定和磁小体生物矿化研究。



郝立凯,1980年生,中国科学院地球化学研究所研究员,博士生导师。2009年获国家留学基金委资助赴德国和丹麦访问学习,2011年获德国DFG资助攻读的博士学位,2014年获国家优秀自费留学生奖学金,2017年获得中国科学院百人计划资助,2018年获

### III

科技部重点研发项目课题资助,2019年获国家自然科学基金面上项目资助。针对重金属与微生物微观作用机制和过程关键科学问题,率先在国际上开展原位微观重金属微生物相互作用的微区分析,建立等电离聚焦-扫描电子显微镜和扫描透射X射线显微镜3D分析技术,实现在单细胞水平高分辨物理结构和化学元素原位微区分析;首次建立荧光标记和激光共聚焦显微镜地球微生物学分析标准,建立金属标记荧光分子库,开展金属微生物地球化学原位微观过程和机理研究;建立荧光探针筛选标准流程,将部分金属荧光探针应用到金属微生物地球化学原位微观分析,实现了重金属微生物地球化学行为的原位立体微观精细刻画。克服以往繁琐复杂的显微镜样品制备过程中对微生物样品微观原位信息的扰动,在最接近原位条件下对重金属微生物地球化学行为和作用机制进行物理结构和化学组成分析,揭示金属和微生物膜及其各组分之间的作用趋势,提高对重金属微生物地球化学微观过程和机制的认识。近期主要研究为重金属环境微生物地球化学原位微观过程和机制,环境分析显微镜学方法和技术构建。发表SCI论文24篇,论文他引500次,高引指数15。



侯振辉,博士,1976年生,中国科学技术大学地球和空间科学学院高级工程师。长期从事激光剥蚀-电感耦合等离子体质谱微区微量元素和同位素分析地球化学研究,探究非基体匹配副矿物定年以及低含

量微量元素分析方法的研发。



谷立新,1988年生,中国科学院地质与地球物理研究所电子显微镜实验室工程师。参与建设了研究所扫描电镜-聚焦离子束-透射电镜显微分析平台,针对地质和地外样品开发了一系列样品制备和分析方法。现主要从事矿物的电子显微学以及月壤颗粒的太空风化作用研究,发表多篇SCI论文和专利。



吴黎光,1994年生,2011年中国地质大学(武汉)本科毕业,现为中国科学院地质与地球物理研究所工程师。吴黎光主要研究独居石的微区U-Th-Pb-Nd-O同位素分析及地质应用。近期的主要成果有:(1)开发了独居石O同位素微区分析的新标样;(2)开发了离子探针测量独居石O同位素的基体效应校正新方法。



李展平,1964年生,清华大学分析中心高级工程师。主要利用俄歇电子能谱(AES)、X射线光电子能谱(XPS)、二次离子质谱(SIMS)等表面分析技术从事固体材料表面分析、结构表征等研究,发表学术论文40多篇。